EUROPEAN ORGANIZATION FOR NUCLEAR RESEARCH
European Laboratory for Particle Physics

sLHC Project

sLHC Project Report 0033

Measurement of the Energy Distribution of the CERN Linac4 160 MeV H^--Beam Close to the PS Booster Injection

K. Hanke, T. Hermanns

Abstract

This report deals with the question, how the mean energy and the energy spread of the CERN Linac4 160 MeV H^--beam can be measured close to the end of the transfer line between Linac4 and PS Booster in the so-called LBS line. The central element of this diagnostics line is a vertical spectrometer magnet, which sorts the particles according to their individual energy along a vertical position axis. From the central value of this distribution the mean energy can be derived, while the width of the distribution is proportional to the beam energy spread.

At first, the method and the simulation tools are briefly introduced. Then, the simulation procedure is explained in detail, which finally leads to a proposal, how the measurement line should look like to determine the energy distribution of the Linac4 beam. Systematic error studies are included as well.

The proposed layout is similar to the present one operating with the CERN Linac2 50 MeV proton-beam. An alternative approach is presented as well. Both are compared and it is suggested to stick to the present layout for the Linac4 line. Finally, the necessary modifications and specifications for the upgrade of the LBS line are summarized.

sLHC-PROJECT-REPORT-0033
23/02/2010

BE-OP
Ref. Linac4

CERN
CH - 1211 Geneva 23
Switzerland

Geneva, 23.02.2010

Table of Contents

1 Introduction

The CERN proton accelerator complex consists of five accelerators, of which the last one is the widely known Large Hadron Collider (LHC). Even if this is the most famous one, it cannot provide high-luminosity beams, if the beams are not well prepared by the pre-accelerators. In the present scheme the first part of the accelerator chain is a linear accelerator, called Linac2, which sends protons with a kinetic energy of 50 MeV to the second machine, the PS Booster. For the ultimate LHC beam the PS Booster must provide particle bunches, containing $2.4 \cdot 10^{12}$ at an normalized emittance of 2.5π mm mrad. These parameters cannot be met as with the present layout. Therefore, in 2013/2014 Linac2 will be replaced by a new linear accelerator Linac4. Then, H^--ions with a kinetic energy of 160 MeV will be sent to the PS Booster. Due to the higher kinetic energy, space charge effects and incoherent tune shift effects will be reduced. Furthermore, a charge-exchange mechanism reduces the losses at the injection point and allows for a more homogeneous filling of the PS Booster acceptance regions. Using this new linear accelerator design it should be possible to provide the required beam parameters in the PS Booster for the ultimate LHC beam.

About 50 m before the beam is injected into the PS Booster the beam can be deflected from the transfer line into a spectrometer line, the *LBS line*. In this line the mean beam energy and the energy spread can be determined. So far this line is tuned for measuring the Linac2 50 MeV proton beam, and for that reason this report addresses the question, how the LBS line must be modified to fulfill the new requirements of measuring the energy distribution of the higher-energetic Linac4 beam, i.e. a mean energy of about 160 MeV and an energy spread of approximately 150 keV. In addition, it is planned to systematically shift the beam energy within ± 1 MeV (energy painting) at the exit of Linac4 to more homogeneously fill the PS Booster acceptance regions. Therefore, a new spectrometer line must be able to resolve these energy shifts as a function of time.

This report starts with a description of the measurement principle, taking the present line as example. Then, simulation studies are summarized (chapter 2) and their results are presented to propose a new, appropriate design for the LBS line (chapter 3). This proposal is analyzed for systematic uncertainties (chapter 4), and finally an alternative proposal in comparison to the present design is briefly introduced (chapter 5). Finally, the report concludes about the main results and summarizes the main elements needed for an LBS line upgrade (chapter 6). Chp. 2 Chp. 3 Chp. 4 Chp. 5 Chp. 6

1.1 The Measurement Principle and General LBS Line Layout

When an ensemble of charged particles traverses a homogeneous magnetic field, the particles are deviated in the field region due to the Lorentz-force depending on their momentum[1]. As particles with the same momentum are equally deviated, a spectrometer magnet sorts them along a spatial axis in the bending plane of the magnet. This is the fundamental physical principle of the spectrometer line. It is obvious that the higher the energy spread of a beam is the larger this spatial distributions becomes.

This spatial distribution is registered by a detector. If the optical design of the spectrometer line and the value of the $\vec{B}$-field of the spectrometer magnet is known, then the central value of the distribution is equivalent to the mean energy value of the beam. In addition, from the geometrical extent of the distribution, the momentum spread can be calculated. The following formula connects the measured beam radius $r_{meas.}$ in the bending plane of the spectrometer magnet with the physical conditions leading to a certain beam radius. It is given by two summands.

$$\begin{aligned} r_{meas.} &= \sqrt{\left(D \cdot \frac{dp}{p}\right)^2 + \beta \cdot \varepsilon} \\ &= D \cdot \frac{dp}{p} \sqrt{1 + \Delta^2} \end{aligned} \qquad (1)$$

$$\text{with } \Delta = \frac{\sqrt{\beta \cdot \varepsilon}}{D \cdot \frac{dp}{p}}$$

where β and ε are beta-function and emittance value at the detector in the bending plane, while D is the dispersion and $\frac{dp}{p}$ is the relative momentum spread of the beam. Only if the beam size is dominated by the summand

[1] The physical method requires to deal with the momentum of a particle rather than with its energy, although the energy distribution of the beam is to be measured. As both are connected through the relativistic invariant mass of the particle, it is equivalent to speak of momentum and to mean energy at the same time. This ambiguity might occur in this report, but whenever numerical values are presented, it is precisely denoted if momentum or energy is meant.

CERN
CH - 1211 Geneva 23
Switzerland

Geneva, 23.02.2010

comprising the momentum spread, the beam momentum spread can be relatively easily measured. Otherwise the two contributions must be disentangled. This requires, that the beam size due to the evolution of the beta function – called *natural beam width* throughout the rest of this report – is small compared to the beam size induced by dispersion, i.e. $\Delta \ll 1$ is only a small perturbation. As the momentum spread is a constant beam property, this can be achieved by generating

1. a large dispersion, i.e. using a strong spectrometer magnet with a significant bending angle,
2. by reducing the emittance value, i.e. absorbing particles in the bending direction by means of a slit, and
3. by installing the detector in a beam waist, i.e. the minimum of the beta-function.

A proposal of a line is considered as reasonable if Δ^2 is of the order of 1%. From equation 1 the relative momentum spread can be calculated, when Δ is negligible and the dispersion value is known at the point where the beam size is measured. Then, from the relativistic relation between total energy E and momentum p the kinetic energy spread dT can be further deduced by

$$\frac{dE}{E} = \beta^2 \cdot \frac{dp}{p} \quad \text{and hence:} \quad dT = \beta \cdot dp. \tag{2}$$

The value for β is 0.52 (H^--ions at kinetic energy $T = 160\,\text{MeV}$).

Fig. 1 In Figure 1 a schematic layout of the present line for the Linac2 beam is shown based on the technical drawings
Ref. [1] in [1] and [2].
Ref. [2]

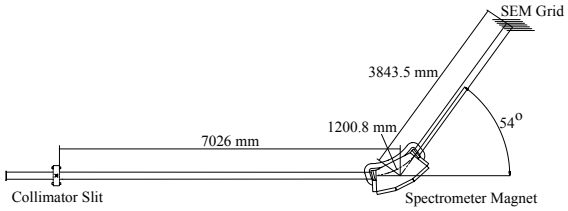

Figure 1: Schematic layout of the LBS line from the slit to the SEM grid. The distances and the bending angle read as they are implemented for Linac2 energy measurements. In front of the slit, not shown in this sketch, the beam is deflected from the transfer line between Linac2 and PS Booster into the LBS line by the LTB.BHZ40 dipole magnet (bending angle 60 mrad) .

For the LBS line the reference plane of measurement is the vertical plane. Therefore the beam is filtered by a vertical slit, before it is analyzed by a vertical spectrometer magnet. This magnet is equipped with non-zero edge angles so that the beam is focused in a waist behind the magnet. At the point of the relative minimum of the beta-function the detector, a SEM[2] grid, is installed, of which the wires are aligned horizontally to resolve a vertical beam size. In the following the simulation tools are described, which are used to determine the new layout for the LBS line.

1.2 Overview about Simulation and Data Analysis Tools

Ref. [3] For the simulation studies two programs are used: *TRACE 3-D* [3] and *Path* [4]. Both programs simulate H^--
Ref. [4] ions with mass $m = 939.294\,\text{MeV}$ and charge $q = -1e$. Furthermore, to respect electromagnetic interactions between the charged particles, the maximum expected beam current of 65 mA is set.

The program Path allows for multi-particle tracking through a beam line. The output of simulations of the transfer line to the entrance of the bending magnet LTB.BHZ40 is taken as input for the LBS line examinations[3]. The data-set contains 42610 H^--ions interacting electromagnetically. In order to reduce the computing time, the beam is separated into uniformly charged rings to approximate the space charge effects instead of considering particle-by-particle interactions. The TRACE 3-D code models a beam as an uniformly filled ellipsoid propagating a 5σ-beam envelope through the beam line with all phase space planes being decoupled. By setting a

[2] **S**econdary **E**mission **M**onitor.
[3] The input beam parameters have been provided by the Linac4 beam dynamics working group.

CERN
CH - 1211 Geneva 23
Switzerland

Geneva, 23.02.2010

non-zero input value for the beam current, a homogeneous charge density within the ellipsoid is assumed, so that space charge effects are approximatively treated as well.

In contrast to Path, slit objects are not implemented in TRACE 3-D and therefore the simulation process is separated into three steps. At first, the new beam line between the LTB.BHZ40 and the slit is implemented in Path to determine the beam parameters behind the slit. These parameters serve as input for TRACE 3-D, so that a geometrical and optical layout of the line behind the slit can be found, where according to equation 1 the SEM grid is located at the minimum of the vertical beta function. Finally, the TRACE 3-D line design is completed between the slit and the SEM grid in Path as well.

The not yet existing experimental data of the SEM grid are taken from Path. The main interest lies in energy and vertical position of the particles at the SEM grid position. These information are input to the data-analysis done with a ROOT-macro [5]. The readout with discrete wires of a SEM grid is simulated, and the resulting Ref. [5]
histogram is fitted to extract the mean energy value and the vertical beam radius $r_{meas.}$. By means of equations 1 and 2 the momentum and energy spread of the Linac4 beam can be calculated. The required value for the vertical dispersion is provided by TRACE 3-D. Once Linac4 will be operating, the beam size simulations with Path will be replace by experimental SEM grid data, which then serve as input to the data-analysis.

For systematic studies respecting alignment errors and simulating manufacturing uncertainties mainly Path is used. Only the systematic error on the dispersion values is estimated with TRACE 3-D.

2 Simulations

The insertion of a slit into the LBS line absorbs particles so that at the SEM grid position only the energy distribution of these particles is measured, which are transmitted through the aperture of the slit. Therefore, in Figure 2 the energy distribution of the Linac4 beam at the entrance of the LTB.BHZ40 dipole magnet, at the exit Fig. 2
of the slit, and at the SEM grid position are depicted, to illustrate the reference distributions, which are subject to the LBS line simulations.

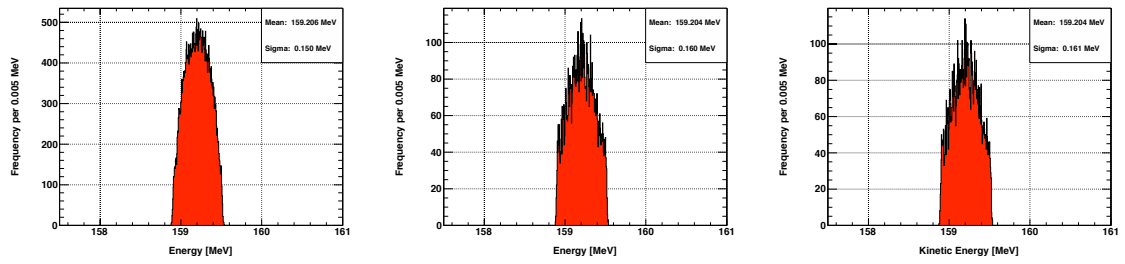

(a) Entrance to LTB.BHZ40 **(b)** Exit of Slit **(c)** SEM Grid

Figure 2: Input energy profile at the entrance to the LBS line (a), behind the slit (b), and at the SEM grid position (c). The mean energy value well coincide, but the energy spread increases. All distributions can be reasonably approximated by a second order polynomial. The data for (b) and (c) already base on a line layout, which will be proposed in chapter 3.

The mean energy values remains almost constant between $159.206\,\mathrm{MeV}$ and $159.204\,\mathrm{MeV}$, while the energy spread (RMS width) increases from $149.6\,\mathrm{keV}$ for the position of LTB.BHZ40 to $159.9\,\mathrm{keV}$ for the slit exit, and $160.6\,\mathrm{keV}$ at the SEM grid. This indicates that the slit slightly affects the energy spread. However, about 20% of the increase between LTB.BHZ40 and slit is already accumulated up to the entrance of the slit. This and also the further increase between slit and SEM grid agree with observations obtained for simulations of the beam evolution along the transfer line [6], which assign the increase to space charge forces. Ref. [6]

Therefore, for the present simulations the reference point for comparison between input and reconstructed values for mean energy and energy spread is defined at the position of the SEM grid, and if the energy spread at the entrance of LTB.BHZ40 shall be determined, a correction of -6.8% must be applied.

Then, it must be guaranteed that the slit does not bias the measurement by selecting a beam slice, which does not represent the full energy distribution. Therefore, vertical position and particle energy must be uncorrelated at the entrance of the slit. The dedicated distribution is illustrated in Figure 3. Fig. 3

The distribution has a correlation coefficient of only 0.4% and hence, the measurement is not biased.

CERN
CH - 1211 Geneva 23
Switzerland

Geneva, 23.02.2010

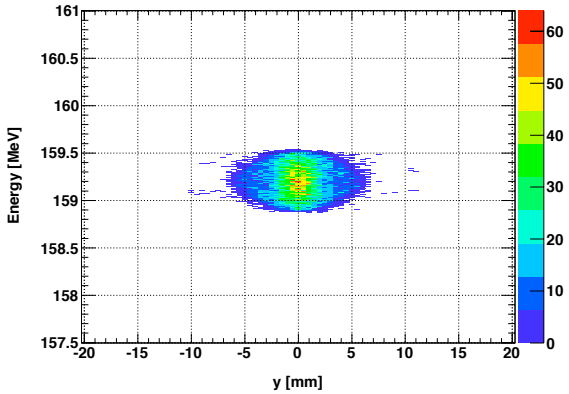

Figure 3: Correlation between energy and vertical position of particles at the slit entrance.

In the following, this chapter deals with the LBS line simulations and their results to find a new design appro-
Chp. 1.2 priate for Linac4 operation. As explained in chapter 1.2, the simulation is divided into several parts because of the need to change from Path simulations to TRACE 3-D and back.

2.1 Line Section 1 – LTB.BHZ40 to Slit with Path

This section deals with the first part of the LBS line simulations where the beam is propagated from the entrance of the dipole magnet LTB.BHZ40 to the exit of the slit. The input parameters for this step describe the particle
Tab. 1 distributions in the three phase space planes. In summary, the beam ellipse parameters are listed Table 1.

	α	β	ε^{1RMS}
horizontal	-0.211	5.357 mm/mrad	0.657 mm mrad
vertical	2.520	22.978 mm/mrad	0.749 mm mrad
longitudinal	15.209	4.038 deg/keV	388.833 deg keV

Table 1: Input parameters for the LBS line simulations with Path. The input beam parameters have been provided by the Linac4 beam dynamics working group.

The particles are tracked with Path through the LTB.BHZ40 magnet. This is an rectangular magnet with length 900 mm and deflection angle 60 mrad. Edge angle focusing and fringe field corrections are applied, by setting the entrance edge angle to $0°$ (only fringe fields), and the exit edge angle to 60 mrad (focusing and fringe field). The reference point of all lengths in the LBS line is defined at the entrance to the magnet. Therefore, downstream the line at position 4089 mm the entrance of the slit is located. Because of space constraints in the experimental zone the slit is positioned at the same location as for the Linac2 LBS line. But due to the higher-energetic Linac4 beam the longitudinal extension must be sufficiently long to stop the particles hitting the absorber material. This slit length can increase to several centimeters for low density materials like carbon, which therefore is a favored reference material for absorptive devices because it is less heavily activated by incident ions than metals. For H^--ions with a kinetic energy of 160 MeV the absorption length is about 85 mm in carbon.

Slit Approximation in Path

In Path, the rectangular entrance area of the slit is defined with horizontal and vertical apertures of 148 mm and 1 mm, respectively. The horizontal value corresponds to the size of the beam pipe, while the vertical value is effectively used to reduce the vertical emittance. By definition, all particles are absorbed that geometrically do not fit into the slit aperture. In order to implement the finite longitudinal length of the slit, a drift distance of 200 mm is inserted and a second exit slit of the same dimension as before is implemented. All particles, which pass the entrance gate, but drift between entrance and exit so that they miss the exit gate, are absorbed. The length of the slit is chosen such that a safety margin for particle absorption in carbon is included. However,

CERN
CH - 1211 Geneva 23
Switzerland

the final length and the choice of material is subject to proper simulations, so that the line layout can change slightly. Thus, the influence of different lengths on the particle distribution behind the slit is studied later on in chapter 4.4.1. Chp. 4.4.1

The described modeling of the slit is a valid approximation because in reality each H^--ion not passing through the slit aperture is either completely absorbed or its electrons are stripped by interactions with the slit material. These stripped particles are filtered out by the spectrometer magnet further downstream. It is obvious that the fraction of these particles lost in the spectrometer magnet must be kept low because they provoke an uncontrolled activation of the spectrometer magnet, its infrastructure, or of the experimental area.

Beam Parameters at the Slit Exit and Input Distributions for TRACE 3-D

In total, 34091 out of 42610 H^--ions, i.e. 80.01%, are absorbed by the slit, corresponding to a transmitted current of 13.00 mA. The remaining particles, revealed in Table 2, determine the beam parameters at the slit exit. They are used to derive the input distribution for the subsequent TRACE 3-D simulation. Tab. 2

	α	β	ε^{RMS}
horizontal	-1.319	12.695 mm/mrad	0.700 mm mrad
vertical	0.026	0.883 mm/mrad	0.086 mm mrad
longitudinal	17.146	4.683 deg/keV	405.671 deg keV

Table 2: Path beam parameters behind the slit.

These parameters cannot be taken immediately as input values for TRACE 3-D simulations. Even though they describe a beam of 1 mm vertical width in Path, the corresponding width in TRACE 3-D would be

$$2 \cdot r_V = 2 \cdot \sqrt{\beta_V \cdot \varepsilon_V^{5RMS}} \approx 2 \cdot 0.61\,\text{mm} = 1.22\,\text{mm} > 1\,\text{mm}. \tag{3}$$

As TRACE 3-D beams are described by emittance values equivalent to 5 RMS, the RMS emittance must be multiplied by 5 to correctly change between the simulation programs. The additional factor 2 accounts for the difference between the full beam size and the beam radius expressed by r.

It can be observed, that this transition leads to a the beam size in the vertical plane, which is too large by about 22%, if the original Path beam parameters behind the slit are directly used as input for TRACE 3-D studies. The problem is related to the fact, that the particle distribution behind the slit are represented by ellipses, which do not precisely model a rectangular slit aperture in the xy-plane. Nevertheless, the Path parameters in the vertical plane can be manipulated such that after the transition in TRACE 3-D the correct vertical slit aperture is obtained. For that reason the 1145 outermost particles from the ensemble are removed, which leads to a smaller vertical emittance, while the orientation of the ellipse is not changed. It can be seen in Figure 4, that these new beam parameters represent a beam with a vertical width of 1 mm. Fig. 4

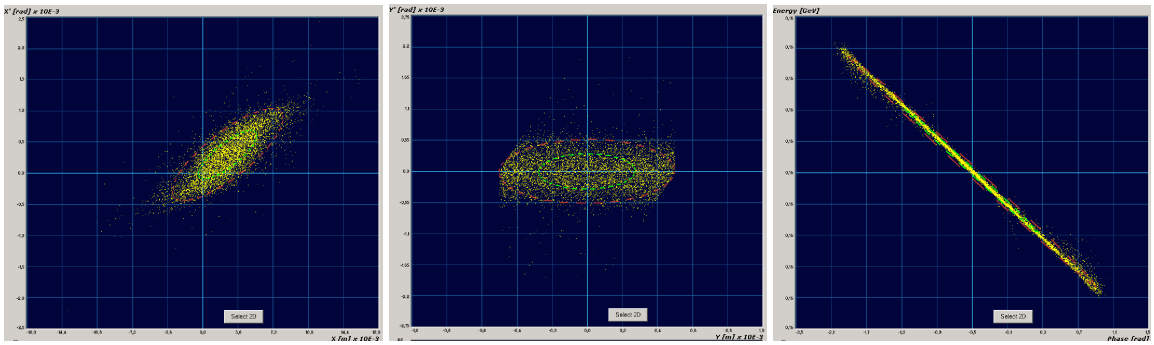

(a) Horizontal Phase Space **(b)** Vertical Phase Space **(c)** Longitudinal Phase Space

Figure 4: Phase space distributions behind slit (screenshots from Path). The yellow points describe the remaining particles not absorbed by slit. In green the nominal 1 RMS ellipse and in red the 86.6% ellipse are drawn, too.

CERN
CH - 1211 Geneva 23
Switzerland

Geneva, 23.02.2010

The scattered histograms show the entire particle distribution behind the slit, while the RMS ellipse is drawn is green and the red trajctory characterizes a 86.6%-ellipse. Deleting about 13.4% of all particles does not too severly affect the distibutions, because only the edges of the phase space distibutions are not well desribed anymore. In contrast, the red ellipses fit now very well to a TRACE 3-D-beam of 1 mm vertical diameter (Table 3).

Tab. 3

	α	β	$\varepsilon^{86.6\%}$
horizontal	-1.319	12.695 mm/mrad	2.525 mm mrad
vertical	0.026	0.883 mm/mrad	0.283 mm mrad
longitudinal	17.146	4.683 deg/keV	1389.880 deg keV

Table 3: TRACE 3-D input parameters derived from phase space distributions behind the slit with Path simulations. The 86.6% emittance values of Path become the 5 RMS values in TRACE 3-D.

The beam current input value for TRACE 3-D is also modified by removing 13.4% of all particles from the ensemble behind the slit. The new value is

$$I = 65.0\,\text{mA} \cdot \underbrace{20.0\%}_{\text{Slit Transmission}} \cdot \underbrace{86.6\%}_{\text{Ellipse Approximation}} \approx 11.25\,\text{mA}. \tag{4}$$

2.2 Line Section 2 – Slit to SEM Grid with TRACE3-D

From equation 1 it can be seen, that the contribution of the natural beam size to the total beam width should be as low as possible if it should be neglected for the energy measurement. Therefore, the line is designed in two steps. At first, a monochromatic beam is simulated, meaning that the energy spread is artificially eliminated, and a set of line parameters is chosen such that behind the spectrometer magnet a local minimum of the vertical beta function is generated. This location is chosen for the SEM grid, because the natural beam width is lowest at this point. In the second step the nominal beam with non-zero energy spread is simulated with this setup and the beam size at the SEM grid position is determined. One figure of merit for a certain line setup is given by the ratio of the total to the natural beam size. The greater this number is, the smaller the perturbation coefficient Δ becomes. In addition, the pure line geometry determines the energy resolution of the spectrometer line. Only these layout are sensible to investigate, which allow for resolving the 160 keV energy spread of the Linac4 beam.

Method of Simulating of a Monochromatic Beam

Tab. 3

Starting from the input values of Table 3 the simulations for the monochromatic beam are performed. A beam with no energy spread can in principle be produced if the longitudinal emittance ε_L is set to a very small value[4]. However, simply setting $\varepsilon_L \approx 0$ contracts the beam in the phase coordinate, too. Hence, the beam size is extraordinarily diminished and electromagnetic repulsion blows the beam up. Thus, the beam length, which is equivalent to the phase Φ, must be kept constant.

From the TRACE 3-D input parameters the nominal longitudinal extension (RMS) of the non-manipulated beam can be calculated.

$$\begin{aligned} \Phi_{max} &= \sqrt{\beta_L \cdot \varepsilon_L^{86.6}} &&\approx 80.7^\circ \\ E_{max} &= \sqrt{\tfrac{1+\alpha_L}{\beta_L} \cdot \varepsilon_L^{86.6}} &&\approx 295.9\,\text{keV} \end{aligned} \tag{5}$$

Furthermore, solving these two equations for β_L and ε_L with α_L as free parameter and $\Phi_{max} \approx 80.7^\circ$ allows for calculating longitudinal beam parameters to arbitrary values of E_{max}. Therefore, choosing $\alpha_L = 0$ gives as a function of the energy spread E_{max} the following longitudinal input parameters for TRACE 3-D simulations.

[4] It cannot be exactly zero due to routines in TRACE 3-D, where the longitudinal emittance enters in the denominator.

CERN
CH - 1211 Geneva 23
Switzerland

Geneva, 23.02.2010

$$
\begin{array}{llllllllll}
(1) & E_{max} & = & 10\,\text{eV}: & \beta_L & = & 8067.718\,\text{deg/keV} & \varepsilon_L & = & 0.807\,\text{deg keV} \\
(2) & E_{max} & = & 75\,\text{keV}: & \beta_L & = & 1.076\,\text{deg/keV} & \varepsilon_L & = & 6050.789\,\text{deg keV} \\
(3) & E_{max} & = & 150\,\text{keV}: & \beta_L & = & 0.538\,\text{deg/keV} & \varepsilon_L & = & 12101.578\,\text{deg keV} \\
(4) & E_{max} & = & 300\,\text{keV}: & \beta_L & = & 0.269\,\text{deg/keV} & \varepsilon_L & = & 24203.155\,\text{deg keV}
\end{array} \tag{6}
$$

The first line represents the monochromatic beam, and the steps with $E_{max} = 75\,\text{keV}$ and $E_{max} = 150\,\text{keV}$ are considered to visualize the evolution of the beam size with increasing energy spread. The maximum energy in (4) has nearly the same value as for the nominal beam without arbitrarily setting $\alpha_L = 0$.

Simulations of Different Beam Line Layouts

For the line layout established for the Linac2 $50\,\text{MeV}$ proton beam, there is a drift space of $6438\,\text{mm}$ between slit and spectrometer magnet. This magnet has a radius of $1200.8\,\text{mm}$ (equivalent to $B = 1.586\,\text{T}$) and a bending angle of $54°$. Its entrance pole is inclined by $14.5°$, and the exit edge angle is $10.5°$. The SEM grid is placed $3101\,\text{mm}$ behind the exit of the magnet. For this geometry, the minimum of the vertical beta-function of the Linac4 beam lies already very close to the present position of the SEM grid, but nevertheless the line must be altered, because the spectrometer magnet does not fulfill the requirements to bend the higher-energetic beam towards the SEM grid.

Seven different scenarios have been studied to investigate how possible modifications of the line affect the energy measurement. The ratio between total beam width and natural beam width and the line resolution are considered to compare the seven types. In the following list per item only the modifications with respect to the above presented Linac2 setup are mentioned. Except for scenario (1) all options are optimized so that the SEM grid is installed in the minimum of the vertical beta-function.

(1) No changes.

(2) Distance between magnet and SEM grid reduced to 3000 mm.

(3) Set entrance edge angle of spectrometer magnet to 15.0°.

(4) Set exit edge angle of spectrometer magnet to 11.0°.

(5) The mid-point of the spectrometer magnet and the SEM grid are kept at their positions as described in the default configuration, but the entrance and exit edge angles of the spectrometer magnet are set to 0°. In order to achieve a focusing effect the radius of the magnet is increased to 1985 mm (equivalent to $B = 0.960\,\text{T}$) and the distance between slit and entrance of the magnet is set to 6039 mm, while the distance between spectrometer magnet and SEM grid is reduced to 2702 mm.

(6) The mid-point of the spectrometer magnet is shifted 1000 mm upstream,while the SEM grid is kept at its position. This gives a new bending angle of 43°. The entrance and exit edge angles of the spectrometer magnet are set to 0°. Hence, the magnet radius is changed to 1775 mm (equivalent to $B = 1.073\,\text{T}$), and so the distance between slit and entrance of the magnet must be adjusted to 5345 mm, and the distance between spectrometer magnet and SEM grid is increased to 3673 mm.

(7) The mid-point of the spectrometer magnet is shifted 1000 mm downstream, while the SEM grid is kept at its position. This gives a new bending angle of 68°. The entrance and exit edge angles of the spectrometer magnet are set to 0°. Hence, the magnet radius is changed to 2150 mm (equivalent to $B = 0.886T\,\text{T}$), and so the distance between slit and entrance of the magnet must be adjusted to 6589 mm, and the distance between spectrometer magnet and SEM grid is increased to 1766 mm.

Simulation Results of the Different Beam Line Layouts

For all scenarios and each of the four values of maximum energy spread the beam sizes ($\sqrt{5}$ RMS) are plotted in Figure 5, as well as the beam sizes scaled to the beam size at $E_{max} = 10\,\text{eV} \approx 0$. The measurement error for a single beam size is set to 7.5%[5]. Fig. 5

[5]The error scale is set for a typical beam size of 3 mm. Its relative value is about 7.5% assuming derived from a simple readout with $0.75\,\text{mm}$ precision and resolution $0.75\,\text{mm}/\sqrt{12}$.

CERN
CH - 1211 Geneva 23
Switzerland

Geneva, 23.02.2010

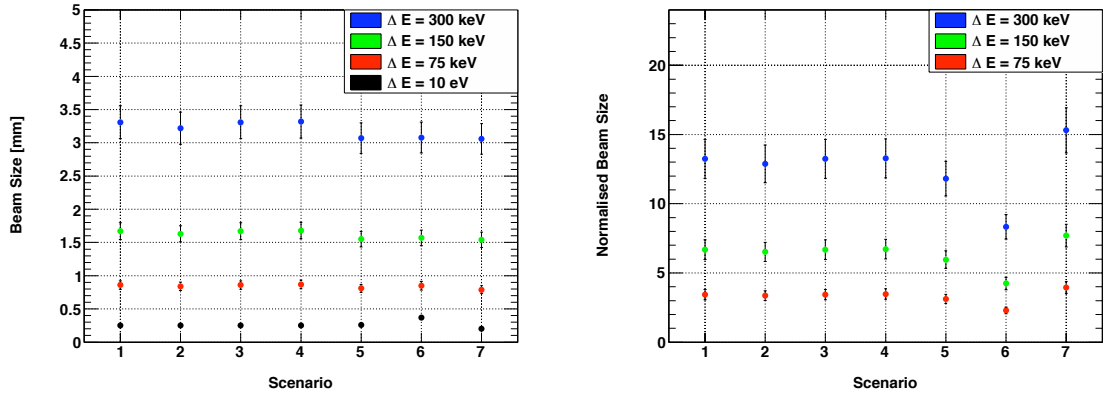

(a) $\sqrt{5}$ RMS Beam Size **(b)** Beam Size Ratio

Figure 5: Beam size ($\sqrt{5}$ RMS) for the seven scenarios (left) and beam size ratio, scaled to the beam size at $E_{max} = 10\,\text{eV} \approx 0$ (right).

The beam size ratio R determines if a scenario is favored or not, because according to equation 1 R is related to the perturbation coefficient Δ

$$R = \frac{r_{meas.}}{\sqrt{\beta \cdot \varepsilon}} = \sqrt{1 + \left(\frac{1}{\Delta}\right)^2} \tag{7}$$

Hence, if the ratio becomes large then Δ becomes small, for instance for $R = 10$ one achieves $\Delta = 0.1$ and so the perturbation Δ^2 is only about 1%.

Comparing all scenarios, the natural beam width and the beam size ratio are strongly influenced by the bending angle of the spectrometer magnet. Increasing the angle further reduces the perturbation Δ (scenario (7)), while a smaller angle degrades the decoupling from the perturbation (scenario (6)). Modifications of edge angles, magnet radius and SEM grid position have less significant influence, but allow for fine-tuning a certain scenario (scenarios (2)-(5)).

The choice of scenario is not only influenced by a low perturbation coefficient, but also a good resolution of the SEM grid must be achieved. The relation between angular resolution $d\varphi$ and momentum resolution dp using a magnet with bending angle φ, of which the mid-point is separated from a SEM grid by the distance L and SEM grid wire spacing s, is given by

$$\frac{dp}{p} = \frac{1}{1 - \frac{d\varphi}{\varphi}} - 1 \quad \text{with} \quad \tan d\varphi = \frac{s}{L}. \tag{8}$$

This can be further transformed into a kinetic energy resolution because

$$\frac{dp}{p} = \frac{\gamma}{1+\gamma}\frac{dT}{T} \quad \text{with} \quad \gamma = 1.169. \tag{9}$$

Following a rule-of-thumb to have five measurement points per full width of a distribution (equivalent to 2σ), an energy resolution of 60 keV between two wires next to each other is required to resolve the Linac4 energy spread of $150 - 160$ keV (1σ-value). For the seven scenarios the resolutions are presented in Table 4.

Tab. 4

The differences between the scenarios are very small, but in general the resolution becomes worse if the distance L is diminished in case of a constant bending angle (compare scenarios (1) and (2)). Nevertheless, a variation of the angle can compensate this decrease, which can be understood when scenarios (5), (6) and (7) are considered. Even if L is lowest for scenario (7) the significant increase in the value of the bending angle over-compensates this, and the best resolution values are achieved.

In general, it can be concluded that the required resolution can be achieved with technically not too challenging parameters for the SEM grid wire clearance, if the bending angle of the spectrometer magnet is large. In this

CERN
CH - 1211 Geneva 23
Switzerland

Geneva, 23.02.2010

Scenario	(1)	(2)	(3)	(4)	(5)	(6)	(7)
L [mm]	3713	3612	3713	3713	3713	4378	3227
φ [°]	54	54	54	54	54	43	68
d = 1.00 mm	84.4 keV	86.8 keV	84.4 keV	84.4 keV	84.4 keV	89.9 keV	77.1 keV
d = 0.50 mm	42.2 keV	43.4 keV	42.2 keV	42.2 keV	42.2 keV	45.0 keV	38.6 keV
d = 0.35 mm	29.5 keV	30.4 keV	29.5 keV	29.5 keV	29.5 keV	31.5 keV	27.0 keV

Table 4: Energy resolution for the seven scenarios for SEM grid wire distances 1.0 mm, 0.5 mm, and 0.35 mm. The clearance of 0.35 mm is the present technical limit what can be manufactured. The length between mid-point of spectrometer magnet (bending angle φ) and SEM grid is given by L.

case the natural beam width and therefore the perturbation coefficient is smallest as well. However then, the geometrical radius of the magnet becomes large, and more material is needed to produce the magnet, so that it becomes more expensive compared to magnets with lower bending angles. A good compromise is therefore to stick to the present bending angle and to improve the resolution by increasing the drift length to the SEM grid. This is advantageous for the SEM grid fabrication, too, because for the wire clearance an appropriate value for 60 keV must be chosen. As the beam size defines the area, which must be covered by the SEM grid, a finer readout demands more readout channels and so more electronics, which determine the main costs for a SEM grid. Hence, a longer drift distance allows for choosing a greater wire spacing and less channels are necessary.

At last, it is briefly reviewed if the vertical beam sizes of the artificial beams choosing $\alpha_L = 0$ fit to the nominal beam sizes with $\alpha_L = 17.146$. Only if these values agree this choice is acceptable and the results can be compared. Hence, in TRACE 3-D the beam sizes for $\alpha_L = 0$ and $E_{max} = 300$ keV are checked against the nominal beam sizes for $\alpha_L = 17.146$ and $E_{max} = 295.9$ keV. The results are summarized in Table 5. Tab. 5

Scenario	(1)	(2)	(3)	(4)	(5)	(6)	(7)
$E_{max} = 300$ keV	3.31 mm	3.22 mm	3.31 mm	3.32 mm	3.07 mm	3.08 mm	3.06 mm
Nominal Beam	3.28 mm	3.19 mm	3.28 mm	3.29 mm	3.04 mm	3.01 mm	3.03 mm

Table 5: Beam size ($\sqrt{5}$-RMS) for the seven scenarios for the approximation with $E_{max} = 300$ keV and $\alpha_L = 0$ compared to the nominal beam with $E_{max} = 295.9$ keV and $\alpha_L = 17.146$.

For all seven scenarios no significant difference can be observed, and thus it is concluded that the choice $\alpha_L = 0$ is valid to obtain reliable results.

2.3 Line Section 2 – Slit to SEM Grid with Path

Before a final design of the spectrometer line is proposed, the seven scenarios of chapter 2.2 designed with TRACE 3-D are investigated in Path as well. Using TRACE 3-D is mandatory to create a certain design of the LBS line, but it must be verified that all approximations made do not falsify the results, such that a tracking code, which is closer to reality, would give completely different results. The way to address this question is to implement each of the seven scenarios in Path, to determine the beam parameters at the SEM grid position, and compare the values of TRACE 3-D and Path simulations. Chp. 2.2

For the Path simulations the particle distributions at the exit of the slit serve as input for the studies. At first, the data-set is duplicated and in one version the relative momentum spread is manually set to $\frac{dp}{p} = 0$, to be able to get the natural beam sizes. Then, the beam sizes corresponding to the beam ellipses for 86.6% and 5 RMS vertical emittance values are determined, the beam size ratios between nominal beam and beam without energy spread are calculated, and these ratios are compared to the results from TRACE 3-D. The dedicated plots are presented in Figure 6. Fig. 6

From the values of the beam size ratio depending on the scenario it can be confirmed with Path that the perturbation strongly depends on the bending angle of the spectrometer magnet, and is only marginally shifted by magnet modifications like varying the edge angles. In addition, even though the beam sizes differ for the two emittance values, the ratio is found to be almost constant. Contemplating the beam size ratios obtained from Path and TRACE 3-D, it is proven that they coincide very well within the range of the error bars. The largest

CERN
CH - 1211 Geneva 23
Switzerland

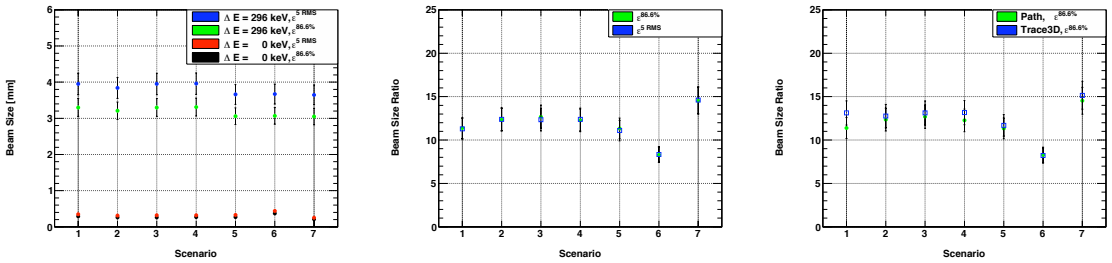

(a) $\sqrt{5}$ RMS Beam Size (Path) **(b)** Beam Size Ratio (Path) **(c)** Ratios from Path and TRACE 3-D

Figure 6: Path beam sizes ($\sqrt{5}$ RMS) for two vertical emittance and two energy spread values (left), the ratio of beam sizes for the two emittance values (middle), and a comparison of beam size ratios obtained from Path and TRACE 3-D for $\varepsilon^{86.6\%}$ (right).

deviation occurs for scenario (A), which is not optimized for having the SEM grid at the minimum of the beta-function in contrast to all other scenarios. Hence, the results from TRACE 3-D simulations can be taken and transferred to Path for a reliable design of the LBS line.

3 Upgrade Proposal for the LBS Line Layout with Linac4 Operation

Chp. 2 From what could be learned from chapter 2, the following upgrade proposal for the LBS line layout with Linac4 operation is given below. Here only the minimal set of parameters, required for the simulation process, are mentioned. Further details and specification, including information about the technical infrastructure, are given
Chp. 6 in the summary of this report in chapter 6.

- **LTB.BHZ40**
  The bending magnet, which deflects the beam into the LBS line, need not be exchanged. It is simulated as a rectangular bending magnet of length 900 mm and with a deflection angle of 60 mrad. The corresponding radius in TRACE 3-D is 15000 mm. The entrance edge angle is $0°$, while the exit edge angle is 60 mrad. Both edge angles are set, so that fringe field corrections are included in the simulations.

- **Slit**
  The position of the slit is proposed to be 4089 mm downstream of the exit of LTB.BHZ40. The vertical aperture is 1 mm, while the horizontal aperture is 148 mm, corresponding to the size of the present beam pipe. The length is currently assumed to be 200 mm, but still subject to a slit design study. It will be proven that this vertical aperture is sufficiently low to keep the contribution of the natural beam size to the total beam size at the level of 1%.

- **Spectrometer Magnet**
  For the spectrometer magnet a compromise between bending angle, resolution and overall size is chosen. The position of the magnet is 6286 mm behind the exit of the slit. The vertical bending angle is kept at $54°$, while the radius of the magnet is set to 1500 mm (equivalent to $B = 1.27$ T). In order to focus the beam at the position of the SEM grid both edge angles are $10°$. This magnet is still subject to a new design study.

- **SEM Grid**
  It is proposed to install a SEM grid 3375 mm (4139 mm from magnet mid-point) downstream of the exit of the spectrometer magnet with a wire clearance of 0.75 mm. In this configuration the momentum and energy resolutions are 109.5 keV$/c$ and 56.8 keV, respectively. As it will be explained later, the minimum geometrical dimensions must be ± 15 mm.

At the end of the line a beam dump must be installed to safely absorb all particles passing the slit.

CERN
CH - 1211 Geneva 23
Switzerland

Geneva, 23.02.2010

3.1 Simulation Results

The design proposal of the LBS line is implemented in Path and the main results concerning beam sizes are listed in Table 6. Tab. 6

Beam Size for $\frac{dp}{p} = 0$	$0.1644\,\text{mm}$
Nominal Beam Size	$1.9593\,\text{mm}$
Beam Size Ratio	11.9179

Table 6: RMS beam sizes (from Path) and beam size ratio for the design proposal of the LBS line.

This beam size ratio is equivalent to a perturbation coefficient $\Delta = 0.0842$. Hence, the proposed line design is appropriate such that the total beam size is clearly dominated by the energy spread.

As depicted in Figure 7(a) simulations give a strict correlation between energy and vertical position at the position of the SEM grid. The correlation coefficient is -99.7% and the absolute value of the fitted slope is $81.9\,\text{keV}/\,\text{mm}$, which agrees well with the theoretically expected value of $56.8\,\text{keV}/0.75\,\text{mm} = 75.7\,\text{keV}/\,\text{mm}$ (energy resolution according to the line dimensions divided by SEM grid wire clearance). Fig. 7(a)

The bin width for the vertical position axis is adapted to the width of a single SEM grid channel of $0.04\,\text{mm}$. That allows for the determination of the energy distribution of all particles that would be sampled on a single wire. The distribution is not infinitely sharp because due to the its width particles with different energies, leaving the slit at slightly differing vertical positions, can be deflected towards the same wire. From the error bars in Figure 7(b) the energy spread per wire is determined to be $13 - 14\,\text{keV}$ (RMS). This value is a measure for the minimum limit of an intrinsic energy resolution. As this value is about four times lower than the energy resolution of the SEM grid, the overlap of energy distributions of two neighboring wires is only at values beyond 2σ. Fig. 7(b)

The two-dimensional distribution is projected to the position axis and the discrete readout of a SEM grid is simulated. The assumed wire clearance of $0.75\,\text{mm}$ and the wire width of $0.04\,\text{mm}$ are implemented as the bin distance and bin width of the histogram. These data are fitted by a second order polynomial, and the spatial position of the maximum of the parabola is assigned to the kinetic energy $T = 159.204\,\text{MeV}$, which is the known value at the SEM grid position (Figure 7(c)). Repeating this procedure for additional energy values result in a linear calibration curve between vertical beam position and mean beam energy like in Figure 7(d). Fig. 7(c) Fig. 7(d)

The required vertical size of the SEM grid is given by the width of the projected signal, which is $\pm 5\,\text{mm}$ for the simulated energy distribution. In addition, the sensitive area must be large enough to still record the entire beam distribution if it is different from the simulated nominal one. As presented in the next paragraph, shifts of up to $\pm 1\,\text{MeV}$ are foreseen and therefore the minimum vertical SEM grid extension must be $\pm 17\,\text{mm}$.

Longitudinal Painting

The longitudinal painting is a systematic manipulation of the Linac4 beam energy, which allows for filling more homogeneously the longitudinal acceptance region of the PS Booster [7]. Variations within $\pm 1\,\text{MeV}$ are considered, and in the simulations these shifts are imposed to the nominal energy of the particle distribution behind the slit. Ref. [7]

The implications for the LBS line are that the sensitive acceptance region of the SEM grid must be enlarged, because the vertical beam distribution gets an offset. In addition, the time-dependence of these shifts should be resolved, so that the readout electronics must provide time-differentiated output signals. It is foreseen to vary the energy by $2\,\text{MeV}$ in about $10\,\mu\text{s}$ and to resolve each step in time intervals of $1\,\mu\text{s}$ (or $200\,\text{keV}$).

The entire energy calibration curve is presented in Figure 7(d). It can be observed that the energy shifts are linearly transformed into shifts of the beam center on the SEM grid. As expected, the slope of this curve coincides to the slope of the nominal correlation curve between energy and position. The vertical error bars are determined by the nominal energy spread, while the horizontal ones are derived by error propagation from the fit parameter errors of the fitted SEM grid data. A conversion of the maximum position error (for energy shift $+1\,\text{MeV}$) into its energy equivalent yields a value of $148.6\,\text{keV}$. Fig. 7(d)

However, a proper treatment of this last value must respect the limited number of particles in the simulations. For that reason in Figure 8 an expected signal for a SEM grid with wire width $0.1\,\text{mm}$ is shown, as well as the Fig. 8

CERN
CH - 1211 Geneva 23
Switzerland

Geneva, 23.02.2010

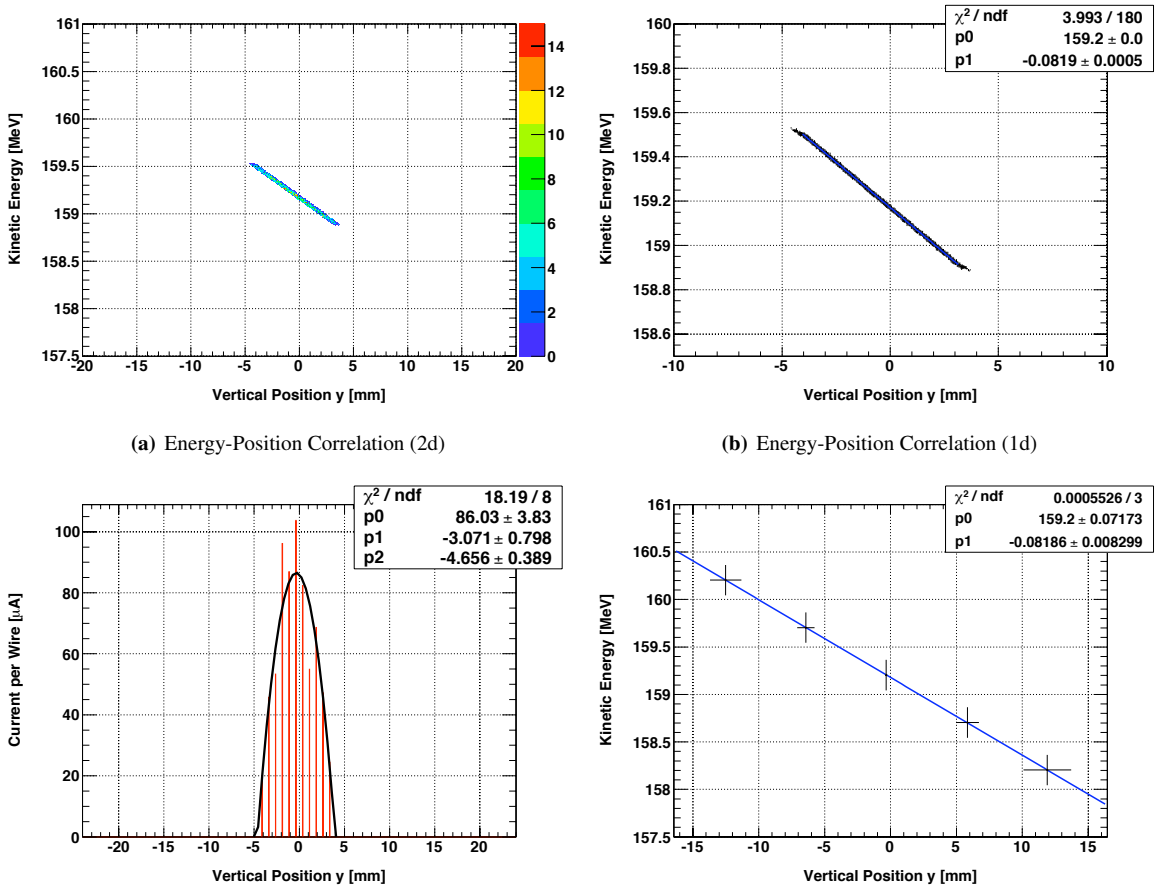

(a) Energy-Position Correlation (2d)

(b) Energy-Position Correlation (1d)

(c) Position Distribution

(d) Energy Calibration Curve

Figure 7: The upper row shows the correlation between energy and vertical position of particles at the SEM grid position (left: 2-dimensional density distribution, right: mean value with RMS error per bin). In the lower row the projection of the two-dimensional distribution to the position axis with a simulation of the discrete SEM grid readout (left), and a linear position calibration curve for beams with shifted kinetic energy values up to ± 1 MeV (right) are displayed.

dedicated energy-position calibration curve.

Through the increase in wire width more data are sampled, statistical fluctuations per wire become less important, and the SEM grid signal follows better the fitted shape. In that case the maximum energy error is reduced to about $89.1\,\mathrm{keV}$ (-40%). An even wider wire of $0.2\,\mathrm{mm}$ results in a maximum energy error of $46.5\,\mathrm{keV}$ (-69%). Therefore, this error is assumed to be an artifact of the limited statistics of the simulations. Later on, in a real measurement the number of particles to be sampled is of the order of 10^{11} instead of $\mathcal{O}(10^3)$ as for these simulations, so that the signal to be fitted should be smooth enough.

Nevertheless, a too large increase of the wire width should be avoided, because the finite width corresponds to an energy spread, too, which is almost $16\,\mathrm{keV}$ for a width of $0.2\,\mathrm{mm}$ (slope of the energy position correlation times wire width, i.e. $81.9\,\mathrm{keV}/\,\mathrm{mm} \cdot 0.2\,\mathrm{mm}$). Any value at this level or above would collect particles from a larger energy interval, so that the good energy resolution of a single wire $(13 - 14\,\mathrm{keV})$ would be spoilt by the too large SEM grid wire width.

Finally, it can be stated that modifications of the wire width influence neither the position of the data points nor the slope of the curve in the energy-position calibration significantly. Existing deviations are very well covered within the range of the errors even for higher sampling statistics, and especially the slope of the calibration curve changes only in the sub-keV range.

CERN
CH - 1211 Geneva 23
Switzerland

Geneva, 23.02.2010

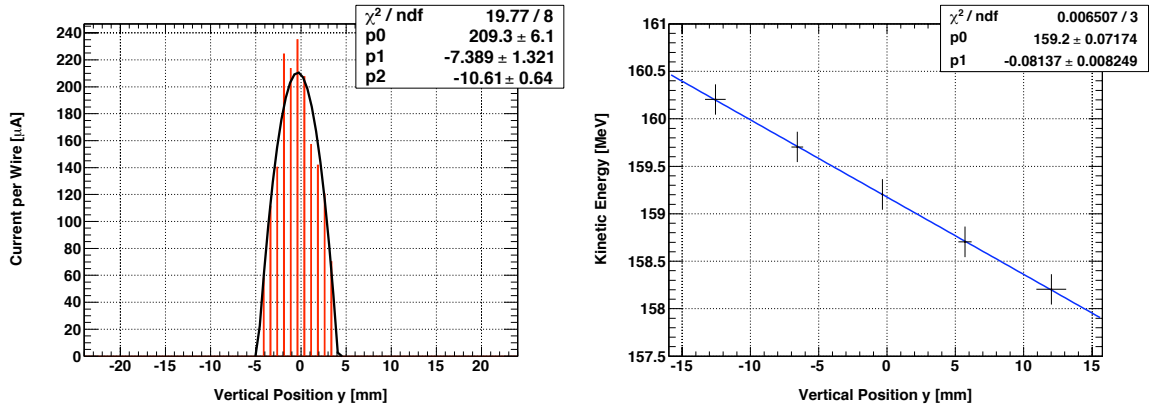

(a) SEM Grid Signal (wire width 0.1 mm)

(b) Energy Calibration Curve (wire width 0.1 mm)

Figure 8: Expected signal seen by a SEM grid with 0.1 mm wire width (left) and energy-position calibration function for this modified SEM grid (right).

3.2 Sensitivity of the SEM Grid

The SEM grid as an electronics device must detect a certain signal per wire to separate it from a noise background. The total integrated signal behind the slit is 13.0 mA, and the SEM grid wires register only 0.7 mA, respectively. For the estimation of the minimum required current transmitted through the slit a minimum signal level per single wire of 55 nA is assumed [8][6]. Ref. [8]

The present SEM grid signal can be scaled down by a factor of about 333, so that the wire with the lowest signal is still above the noise level. Hence, the minimum current transmitted through the slit must be 0.04 mA, equivalent to an intensity of approximately $2.5 \cdot 10^8$ H^--ions per 1 µs. The corresponding minimum beam intensity is $2.5 \cdot 10^{10}$ ions per nominal Linac4 100 µs-bunch prepared for energy measurements.

3.3 Measurement of Beam Size and Determination of Energy Spread

From the measurement of the beam spot on the SEM grid not only the mean energy, but also the energy spread can be derived. In this case, the experimental quantity of interest is the beam size. Because of equation 1 the physical beam property of the momentum (energy) spread can be calculated, if the beam size is measured, given that the local value of the vertical dispersion function is known (from simulations for instance). As for the proposed line layout the perturbation coefficient is small, the equation simplifies to

$$r_{meas.} \approx D \cdot \frac{dp}{p} = \frac{\gamma}{1+\gamma} \cdot D \cdot \frac{dT}{T} \tag{10}$$

The vertical dispersion D is determined locally at the SEM grid position. Its value from TRACE 3-D is

$$D = 3.607\,\text{m}. \tag{11}$$

Taking the beam size read from Path$r_{meas.} = 1.9593$ mm as a simulation of the measurement one obtains for relative momentum spread and absolute energy deviation

$$\frac{dp}{p} = 5.432 \cdot 10^{-4} \quad \text{and} \quad dT = 160.4\,\text{keV}. \tag{12}$$

That is a deviation of -0.2 keV compared to the input value of 160.6 keV at the SEM grid.

Later on, the beam size will be determined from a measured SEM grid signal, and hence it must be extracted from the second order polynomial fit. As it is not a simple fit parameter, a statistical acceptance-rejection method can be used to find the required figure, for instance [9]. For this method pairs of equally distributed random Ref. [9]

[6] This includes already a safety margin of one order of magnitude. That might be a bit too conservative, but given the fact, that no second proper simulation sample is available, this appears to be justified.

CERN
CH - 1211 Geneva 23
Switzerland

Geneva, 23.02.2010

numbers are generated. The first number is distributed along the geometrical extent and the second number is scaled within the detectable current range of the SEM grid, so that with a sufficiently high number of pairs the entire two-dimensional measurement plane of the SEM grid is covered. Then, the fitted boundary curve is overlaid to this plane, and only these pairs of random numbers are accepted, which are enclosed by the curve, otherwise they are rejected. Hence, the continuous distribution of particles is re-simulated, exactly limited by the fitted curve on the experimental data. Finally, the RMS of this distribution along the position axis provides
Fig. 3.3 the value for the beam size (Figure 3.3).

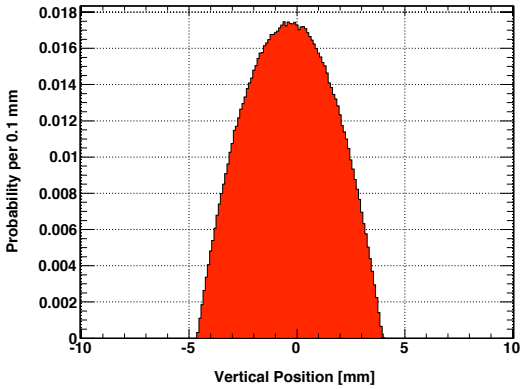

Figure 9: Re-simulated SEM grid signal (normalized). The RMS of the distributions along the vertical position axis gives the value for the beam size (radius).

This reconstruction method is tested with four statistics of random numbers: 10^4, 10^5, 10^6, and 10^7. Each
Tab. 7 setting is averaged over ten runs to estimate a statistical error. The results are listed in Table 7.

Statistics N	Beam Size [mm]	Statistical Error	Deviation	$\frac{dp}{p}$ $[\times 10^{-4}]$	dT [keV]	Deviation
10^4	1.9366	0.92%	-1.2%	5.369	158.6	-1.2%
10^5	1.9294	0.35%	-1.5%	5.349	158.0	-1.6%
10^6	1.9285	0.09%	-1.6%	5.347	157.9	-1.7%
10^7	1.9279	0.04%	-1.6%	5.345	157.9	-1.7%

Table 7: Results for measured beam sizes with the acceptance-rejection method for different statistics of generated random numbers. The statistical error stems from ten iterations of the procedure. For the absolute energy deviation the mean kinetic energy at the SEM grid position of 159.204 MeV is used as input. The deviations are calculated with respect to the Path reference value of 1.9593 mm and $dT = 160.6$ keV, respectively.

The statistical error is of the order $1/\sqrt{N}$. Hence, the more random data are generated the further it can be neglected. On the other hand, the computing time increases as well, and in the end a compromise between required statistical accuracy and accepted computing time must be found. In general, it is obvious that even for the lowest statistics this error is already at or even below the resolution of the position measurement with the SEM grid without a fit, assuming it is given by $\frac{\text{pitch}}{\sqrt{12}} \approx 220\,\mu\text{m}$. In addition, the largest statistical error corresponds to an energy shift of 1.5 keV, which is smaller by one order of magnitude compared to the intrinsic energy width sample on the same wire.

Comparing these results to the Path reference value, an intrinsic systematic error occurs. It can be seen that independently of the statistics the beam size is always lower than the reference size, also refletected in the absolute energy spread values, which must be compared to their reference value of 160.6 keV. The general tendency to obtain better results with lower statistics must be carefully discussed, because even if the worst absolute result is obtained for the highest statistics, it must be considered that the statistical error counterbalances this behaviour. Therefore, it is still recommended to strive for high statistical data samples.

This procedure can be further optimized concerning computing time by constraining the interval of random number to only what is really necessary. For a real application the interval, in which the random numbers are created, can be found dynamically depending on signal height and signal spread on the SEM grid, so that less pairs are rejected as in the above presented example. In addition, parallel computing could be an option, so that

CERN
CH - 1211 Geneva 23
Switzerland

Geneva, 23.02.2010

the ten runs can be simulated at the same time.

4 Uncertainties

In order to exploit the full energy resolution of the SEM grid it is required that the experimental uncertainties of the measurement remain below the design resolution value of $56.8\,\mathrm{keV}$. Besides a statistical error due to the reconstruction method of the beam width, all uncertainties are estimated by imposing alignment and manufacturing errors on the optimal line design.

- The alignment error for slit, spectrometer magnet, and SEM grid is assumed to be $1\,\mathrm{mm}$. Thus, the distances between
  (a) slit and spectrometer magnet, and
  (b) spectrometer magnet and SEM grid
  are varied by $\pm\,2\,\mathrm{mm}$ (maximally unfavored constellation).
- The manufacturing accuracy of the spectrometer entrance and exit edge angles is simulated to be $\pm\,0.5°$.
- The knowledge on the value of the $\vec{B}$-field are allowed to vary by $\pm\,0.1\%$.
- The slit width is varied by $\pm\,5.0\%$, corresponding to an uncertainty of $50\,\mu\mathrm{m}$.

These twelve modifications (one per item with a positive and negative deviation each) are individually introduced in Path to the dedicated elements, and the vertical beam size is re-measured at the position of the SEM grid. Per item the greater deviation of the two from the reference value is taken, and the uncertainty is calculated by the square root of their quadratic sum. Thus, a systematic error is assigned to the measurement of the beam spot on the SEM grid, and consecutively converted into errors on mean energy (by shifts of the mean position) and energy spread (by variations of the beam width). The reference values used in this chapter are summarized in Table 8. Tab. 8

Quantity	Symbol	Reference Value
Beam Size	r	$1.9593\,\mathrm{mm}$
Beam Size Ratio	R	11.9179
Mean Energy	T	$159.204\,\mathrm{MeV}$
Energy Spread	dT	$160.6\,\mathrm{keV}$
Vertical Dispersion	D	$3.607\,\mathrm{m}$
Perturbation Coefficient	Δ	0.0842

Table 8: Summary of reference values for error calculations.

The alignment and manufacturing errors can also be used to determine the degradation of the SEM grid resolution due to changes in the geometrical layout. Furthermore, if they are implemented in the TRACE 3-D layout of the line it is possible to study their effect on the vertical dispersion value. Finally, as for the present study the natural beam width is neglected due to its minor contribution to the total beam size, a systematic error for this approximation can be given as well.

In the second part of this chapter further stability checks of the measurement are performed. Slit length and aperture as well as beam input parameters are varied to verify that the basic concept of the proposed measurement scenario is valid when some main elements and assumptions of the simulation change.

4.1 Error of Mean Energy Measurement

The error on the mean energy measurement comprises of two contributions. The first is determined by the error on the center position of the energy distribution. It is calculated by propagating the uncertainties on the fitted coefficients of the second order polynomial. For the nominal beam the central position on the SEM grid is

CERN
CH - 1211 Geneva 23
Switzerland

$m = -0.2938$ with $\sigma_m = 0.1020\,\text{mm}$. Through the linear calibration curve between position displacement and energy shift with slope $81.9\,\text{keV}/\,\text{mm}$ (Figure 7(b)) it is converted into an energy deviation of $\sigma_T^{fit} = 8.4\,\text{keV}$. Fig. 7(b)

The second error is imposed to the mean energy because the central value of the fit to the SEM grid data is displaced, if the line deviates from its optimal design. Therefore, for each of the above listed error sources an individual SEM grid signal is fitted with a second order polynomial. The quadratic sum over all deviations is $3.4976\,\text{mm}$ or $\sigma_T^{sys.} = 286.5\,\text{keV}$.

In addition, the energy measured on a single wire of $\pm(13-14)\,\text{keV}$ must be added as an intrinsic error, which sets a lower bound on the measurement precision given that all other errors could be suppressed. Therefore, the total error on the mean energy measurement is

$$\sigma_T = \sigma_T^{fit} \oplus \sigma_T^{sys.} \oplus \sigma_T^{intr.} = 286.9\,\text{keV}(287.0\,\text{keV}) \quad \text{and} \quad \frac{\sigma_T}{T} = 1.8 \cdot 10^{-3}$$

The error is dominated by the error on the knowledge of the absolute value of the $\vec{B}$-field of the spectrometer magnet. Therefore, improving this precision by one order of magnitude also diminished the error by almost the same factor. On the other hand, if the energy measurement is calibrated the absolute knowledge is less important but only the fluctuations of the adjusted value and therefore the reproducibility of one measurements concerns. For the latter it is required to obtain a field stability of $\frac{dB}{B} = 2 \cdot 10^{-4}$ to fully exploit the resolution of the SEM grid.

4.2 Error on Energy Spread Measurement

The error on the energy spread measurement can be subdivided into the errors in the beam size measurement, the determination of the vertical dispersion value, and the error on the perturbation coefficient.

Error on Beam Size Measurement

The beam size measurement is subject to two sources of errors. The resolution of the SEM grid, which usually is assumed to be $\frac{p}{\sqrt{12}} = \frac{0.75\,\text{mm}}{\sqrt{12}} = 0.22\,\text{mm}$ or equivalent to a relative error of 11.1%, can be significantly improved, by fitting the data and applying the statistical acceptance-rejection method, to retrieve a beam size from the fit result. This method has an intrinsic systematic error, which is almost constant if a sufficiently high number of random number pair is generated (refer to Table 7 and discussions afterwards). The estimation of this error considers the greatest value of 1.6% for the statistics of 10^7 random number pairs. Tab. 7

$$\sigma_r^{(1)} = 0.0314\,\text{mm} \quad \text{and} \quad \frac{\sigma_r^{(1)}}{r} = 1.6\%.$$

The new absolute energy spread is

$$dT^{(1)} = 157.9\,\text{keV} \quad \text{and} \quad \sigma_{dT}^{(1)} = 2.7\,\text{keV}.$$

The second error on the beam size measurement stems from the above described alignment and manufacturing insufficiencies. An analysis reveals that

$$\sigma_r^{(2)} = 0.0105\,\text{mm} \quad \text{and} \quad \frac{\sigma_r^{(2)}}{r} = 0.5\%,$$

and referred to the reference energy spread

$$\sigma_{dT}^{(2)} = 0.9\,\text{keV}.$$

As these two errors can be considered as independent from each other, the total uncertainty is given by the square root of the quadratic sum of the two terms

$$\sigma_{dT}^{sys.}(r) = \sqrt{\left(\sigma_{dT}^{(1)}\right)^2 + \left(\sigma_{dT}^{(2)}\right)^2} = 2.9\,\text{keV} \quad \text{and} \quad \frac{\sigma_{dT}^{sys.}(r)}{dT} = 1.8\%$$

CERN
CH - 1211 Geneva 23
Switzerland

Geneva, 23.02.2010

If the contribution of the natural beam size is neglected beam size r and relative momentum spread $\frac{dp}{p}$, and therefore the relative energy spread $\frac{dT}{T}$, are proportional to each other. Thus, the relative systematic error for beam size measurement and energy spread are the same and the total error on the beam size can be immediately converted to energy units.

Error on Vertical Dispersion Value

In order to obtain the error on the vertical dispersion value at the SEM grid position, the TRACE 3-D configuration file is modified with respect to the described systematic deviations of the line. It is calculated to be

$$\sigma_D^{sys.} = 0.0126 \quad \text{and} \quad \frac{\sigma_D^{sys.}}{D} = 0.4\%$$

and the systematic error for the kinetic energy spread is

$$\sigma_{dT}^{sys.}(D) = 0.6\,\text{keV} \quad \text{and} \quad \frac{\sigma_{dT}^{sys.}(D)}{dT} = 0.4\%.$$

As before, dispersion and kinetic energy width are proportional so that the relative error on the dispersion is the same as for the kinetic energy width.

Driven by the simulation constraints of TRACE 3-D, the variation of the slit width is not included in this systematic error, because the simulation starts only behind the slit. In principle, it would be possible to vary this parameter in Path to get new input parameter for the TRACE 3-D simulation. However the error in the transition between the two programs is larger than the expected error due to the slit width variation. Therefore, any result would be smeared and dominated by the transition effect. Considering the contribution of slit width variations to the previously studied systematic errors it is reasonable to assume that this is only a minor effect.

At last, it must be noted that the vertical dispersion is derived from a simulation code, so that an intrinsic uncertainty due to the chosen simulation model is included as well. As this cannot be estimated so far, it would be useful to think about an independent simulation method to cross-check the result or to determine the vertical dispersion experimentally. In both cases the model uncertainty can be evaluated.

Error on Perturbation Coefficient Δ

The error on the perturbation coefficient Δ quantifies the validity to neglect the natural beam width correction when calculating the energy spread. It value is given through the error on the beam size ratio R by

$$\sigma_\Delta^{sys.} = \frac{R}{\sqrt{(R^2-1)^3}} \cdot \sigma_R = 0.0064 \quad \text{and} \quad \frac{\sigma_\Delta^{sys.}}{\Delta} = 7.6\%.$$

Even in the most unfavored case of $\Delta + \sigma_\Delta^{sys.} = 0.0906$ the perturbation is 0.8% and so still below 1.0%, because of the quadratic dependence of the momentum spread on this value.

Total Error on Energy Spread

By means of equations 1 and 9 and error propagation the total systematic error on the energy spread can be calculated.

$$\frac{\sigma_{dT}}{dT} = \sqrt{\left(\frac{\sigma_r}{r}\right)^2 + \left(\frac{\sigma_D}{D}\right)^2 + \left(\frac{\Delta^2}{1+\Delta^2}\right)^2 \cdot \left(\frac{\sigma_\Delta}{\Delta}\right)^2} \tag{13}$$

Indicated by the third summand, the relative error of the perturbation coefficient is suppressed by two orders of magnitude with respect to the two other contributions because the pre-factor scales with Δ^2. But as the finite slit width allows for sampling a certain energy distribution with width 13 keV to 14 keV on one wire, this intrinsic error must be added at last. Collecting all figures the total error on the energy spread becomes, neglecting σ_Δ,

CERN
CH - 1211 Geneva 23
Switzerland

Geneva, 23.02.2010

$$\sigma_{dT} = 2.9\,\text{keV} \oplus 0.6\,\text{keV} \oplus 13\,\text{keV}(14\,\text{keV}) = 13.3\,\text{keV}(14.3\,\text{keV}) \quad \text{and} \quad \frac{\sigma_{dT}}{dT} = 8.3\%(8.9\%).$$

The total error is dominated by the intrinsic error, which can only be reduced if the vertical slit aperture is further closed as it will be shown in chapter 4.5. Nevertheless, the total error lies well below the sensitivity of the SEM grid, and thereby it does not significantly influence the precision of the measurement.

Chp. 4.5

Inclusion of Perturbation Coefficient

Finally, it is investigated how the energy spread would be shifted if the perturbation coefficient Δ is included in the calculation. From solving the second line of equation 1 for $\frac{dp}{p}$ including a non-neglible Δ and calculating the energy spread gives

$$dT = 159.9\,\text{keV}$$

using the values for $r_{meas.}$ and Δ as cited in Table 8. This value is subtracted from $dT = 160.4\,\text{keV}$ without the inclusion of Δ

Tab. 8

$$dT(\Delta = 0) - dT(\Delta \ll 1) = 0.5\,\text{keV}$$

Not only compared to the resolution of the SEM grid but also to the systematic error this correction is a lower order effect. In summary, this quantifies that neglecting the perturbation coefficient is well justified.

4.3 Error on SEM Grid Resolution

For the error on the SEM grid resolution the precision of manufacturing the wire distance and the alignment error of SEM grid to spectrometer magnet are taken into account. The wire clearance $s = 0.75\,\text{mm}$ is producible with a typical accuracy of $\sigma_s = 0.1\,\text{mm}$, and the distance between spectrometer magnet and SEM grid $L = 4139\,\text{mm}$ is known up to $\sigma_L = 2\,\text{mm}$. These geometrical errors slightly change the angle $d\varphi$ covered by two adjacent wires with respect to the mid-point of the magnet, and so the momentum/energy resolution of the SEM grid. Using equations 8 and 9 they are propagated to an uncertainty on the SEM grid energy resolution.

$$\sigma_{SEM} = T \cdot \frac{\gamma + 1}{\gamma} \cdot \frac{d\varphi}{\varphi} \cdot \frac{1}{\left(1 - \frac{d\varphi}{\varphi}\right)^2} \sqrt{\frac{\sigma_s^2}{s^2} + \frac{\sigma_L^2}{L^2}} \tag{14}$$

Inserting the above mentioned values and the bending angle of the spectrometer magnet $\varphi = 54°$ gives

$$\sigma_{dT_{SEM}} = 7.6\,\text{keV} \quad \text{and} \quad \frac{\sigma_{dT_{SEM}}}{dT_{SEM}} = 13.3\% \tag{15}$$

As s is much smaller than L and thus $d\varphi \approx s/L = \mathcal{O}(10^{-4})$, the scaling factor in front of the square root term is very low. As the geometrical errors scale with this pre-factor, the nominal two-wire-resolution of $dT_{SEM} = 56.8\,\text{keV}$ is degraded only on a low level. However, the main contribution to this error is determined by the uncertainty of the SEM grid wire distance. The technical limit is reached at an accuracy of $0.01 - 0.02\,\text{mm}$. In that case the error on the SEM grid resolution decreases to $0.8\,\text{keV}$ (1.3%) and $1.5\,\text{keV}$ (2.7%), respectively. Thus, in order to be comparable to the systematic errors presented above one should aim at an accuracy of about $0.04\,\text{mm}$ (3 keV or 5.3%).

4.4 Stability of the Proposed LBS Line Layout

In this subsection three stability checks are examined. At first, the slit length and vertical aperture, and then the input parameters in front of LTB.BHZ40 are varied. These changes could in principle immediately act on the particle distribution behind the slit, which is analyzed by the SEM grid, and therefore the measurement results could be altered.

CERN
CH - 1211 Geneva 23
Switzerland

Geneva, 23.02.2010

4.4.1 Variation of Slit Length

For the present simulation the slit material is assumed to be carbon, so that the length is chosen to be 200 mm. Nevertheless, the conclusions of the LBS line simulations must not depend on the slit length, because its actual length and the choice of material is still subject to simulations. For that reason the slit is simulated with a variety of lengths: 150 mm, 100 mm, 50 mm, and 20 mm. Each of these four new slits is aligned at the point of its exit, so that the distance between LTB.BHZ40 magnet and slit is increasing (4139 mm, 4189 mm, 4239 mm, and 4269 mm). Then, the beam sizes are measured with the SEM grid for a monochromatic beam and the beam with nominal energy spread. All results are shown in Table 9. Tab. 9

Slit Length	Beam Size [mm] $\frac{dp}{p} = 0$	Nominal	Beam Size Ratio	Δ	dE/dy [keV/mm]	dE per wire [keV]	Current [mA]
200 mm	0.1644	1.9593	11.9179	0.0842	81.9	13-14	13.00
150 mm	0.1667	1.9587	11.7499	0.0854	81.9	13-14	13.20
100 mm	0.1692	1.9579	11.5715	0.0867	81.9	13-14	13.41
50 mm	0.1723	1.9586	11.3674	0.0883	81.8	13-14	13.64
20 mm	0.1739	1.9601	11.2714	0.0891	81.8	13-14	13.75

Table 9: Beam sizes, beam size ratio, perturbation coefficient Δ, and transmitted current for slits with different length. The slope of the energy-position calibration curve and the energy spread sample on one wire are mentioned, too. For comparison the reference values for the nominal simulation are repeated in the first line of the table.

A variation of the slit width assuming that it is aligned at its exit position does not significantly influence the perturbation coefficient. It is slightly decreasing, but the total contribution of natural to the total beam size is still below 1%. Furthermore, the transmitted current increases by maximally 5.8% when reducing the slit length to 20 mm. The reason for these slightly different results can be found in the particle propagation. As the slit length is lower, less particles hit the slit in its interior and are absorbed. For the linear calibration relation between vertical position and energy, and for the spread of the energy distribution sampled on wire the changes are negligible.

In summary, the LBS line simulations are very stable with respect to modification of the slit length. In addition, the transmitted current increases only slightly when the length decreases, but this has no considerable effect on the beam dump design at the end of the line.

4.5 Variation of Vertical Slit Width

The vertical slit length is the parameter, by which the beam size ratio R and the perturbation coefficient Δ, the energy spread sampled on one wire, and the transmitted current can be manipulated. Besides the nominal case of 1 mm, slit width of 0.5 mm and 2.0 mm are examined, which represent a sensible interval for potential slit widths. The results are presented in Table 10. Tab. 10

Slit Aperture	Beam Size [mm] $\frac{dp}{p} = 0$	Nominal	Beam Size Ratio	Δ	dE/dy [keV/mm]	dE per wire [keV]	Current [mA]
0.5 mm	0.0888	1.9672	22.1436	0.0452	81.8	7-8	6.11
1.0 mm	0.1644	1.9593	11.9179	0.0842	81.9	13-14	13.20
2.0 mm	0.3188	1.9828	6.2195	0.1629	78.5	26-27	25.55

Table 10: Beam sizes, beam size ratio, perturbation coefficient Δ, and transmitted current for slits with different length. The slope of the energy-position calibration curve and the energy spread sample on one wire are mentioned, too. For comparison the reference values for the nominal simulation are repeated in the second line of the table.

It can be observed that the natural beam width and the energy spread sampled per wire approximately linearly scale with the ratio of the vertical slit widths. As the total beam size remains nearly constant, the beam size ratio and so the perturbation coefficient scales therefore with the inverted factor. This shows, that the intrinsic resolution and the perturbation coefficient of a proposed solution are not independent of the vertical slit aperture. However, these key parameters for a certain solution can be improved if the slit is further closed.

CERN
CH - 1211 Geneva 23
Switzerland

Geneva, 23.02.2010

Finally, it must be noted that any modification of the slit aperture affects the absorption rate. The current transmitted through the slit scales approximately linearly with the vertical slit width. Even if intrinsic resolution and perturbation coefficient can be reduced by further closing the aperture, the transmitted signal must still be high enough to be detected over the noise background on the SEM grid. In addition, if the slit must absorb more particles, of which the energy must be dissipated, the choice of an appropriate material and cooling can become important.

4.5.1 Variation of Beam Input Parameters

One central aspect of the spectrometer line is that the natural beam size can be neglected with respect to the total beam size at the position of the SEM grid. However, the line is optimized for a certain set of input parameters and thus it should be clarified if the design is still appropriate for energy measurements if the beam input parameters change.

Due to the lack of input data-sets with differing beam parameters, the new phase space input distributions are randomly generated in Path following Gaussian distributions, which are initially parameterized by the reference values of the nominal beam. In total, three distributions, are created at the entrance to LTB.BHZ40 and propagated through the LBS line. The statistics comprises 42610 H^--ions and the kinetic energy and initial beam current are the same as in the nominal case. Then, in all three phase space planes the Twiss-parameters α and β and the emittance are subject to modifications. In total, there are nine parameters set to either half or double of its nominal value, so that for 18 input scenarios the effect of the modification can be studied.

Tab. 11 From Table 11 it can be derived that the Gaussian approximation is acceptable. In this table the nominal and the Gaussian beam are compared at the exit of the slit, and the deviations are sufficiently small at a level of about $10 - 15\%$[7].

		Nominal	Gaussian
horizontal	α	-1.319	-1.200
	β [mm/mrad]	12.695	12.481
	ε [mm mrad]	0.700	0.688
vertical	α	0.026	-0.035
	β [mm/mrad]	0.883	0.772
	ε [mm mrad]	0.086	0.094
longitudinal	α	17.146	15.969
	β [deg/keV]	4.683	4.382
	ε [deg keV]	7.080	6.873
Transmitted Current [mA]		12.995	10.677
Vertical Beam Size on SEM Grid [mm]		1.9593	1.8664

Table 11: Comparison between nominal and Gaussian beam data at the exit of the slit. The first column shows the exact values for the nominal beam, while the second column lists the values of the Gaussian approximation.

Varying individual parameters, it becomes immediately obvious that modifications in one plane do not effect Tab. 12 the others. Therefore, only the results for the vertical measurement plane are summarized in Table 12, because that is the measurement plane of interest.

The stability of the results with respect to statistical fluctuations due to the finite number of simulated particles is estimated in the following way. For the nominal Gaussian beam ($\frac{dp}{p} \neq 0$) data are generated ten times and a beam size of (1.8669 ± 0.0096) mm is obtained (relative error 0.5%). It can be observed that each measurement with a modified input beam parameter is already covered by the statistical $2\sigma_r$-interval. For the monochromatic beam the coincidence is less prominent, because the beam size averaged over ten data samples is (0.1618 ± 0.0008) mm (relative error 0.5%).

What concerns the physical performance, the value of the perturbation coefficient well coincide to each other. There is no case where the perturbation is so strongly enhanced, that it cannot be neglected anymore. The slope

[7] This gives also an estimation to which extent the beam is actually described by Gaussian distributions.

CERN
CH - 1211 Geneva 23
Switzerland

	Beam Size [mm]				dE/dy	dE per wire	Current
	$\frac{dp}{p} = 0$	Nominal	Beam Size Ratio	Δ	$[keV/mm]$	$[keV]$	[mA]
α_0, β_0, ε_0	0.1568	1.8664	11.9031	0.0843	81.9	13-14	10.89
$\alpha = 0.5 \cdot \alpha_0$	0.1611	1.8816	11.6797	0.0859	81.8	13-14	7.33
$\alpha = 2.0 \cdot \alpha_0$	0.1464	1.8708	12.7787	0.0785	82.0	12-13	21.29
$\beta = 0.5 \cdot \beta_0$	0.1514	1.8527	12.2371	0.0820	81.9	12-13	16.57
$\beta = 2.0 \cdot \beta_0$	0.1620	1.8713	11.5512	0.0869	82.2	12-13	5.43
$\varepsilon = 0.5 \cdot \varepsilon_0$	0.1577	1.8627	11.8117	0.0850	82.0	12-13	15.57
$\varepsilon = 2.0 \cdot \varepsilon_0$	0.1538	1.8788	12.2159	0.0821	82.1	12-13	7.51

Table 12: Beam sizes, beam size ratio, perturbation coefficient Δ, and transmitted current for slits with different length. The slope of the energy-position calibration curve and the energy spread sample on one wire are mentioned, too. The beam ellipse parameters for the reference beam are indicated by a lower index "0" (first row), later on only the changes with respect to the nominal values are mentioned.

of the energy-position calibration curve is nearly unchanged, and the same is true for the energy spread sampled on the same wire. In that sense, the slit acts as a kind of equalizer, so that the variations at the beginning of the line are smeared out.

In contrast, the value of the transmitted current varies significantly. This does not really influence the actual design of the measurement line, but only the simulations of the slit and of the beam dump at the end of the line. A possible solution to overcome this effect could be to built a slit with variable vertical aperture. In case of the high transmission scenarios, it can be closed further to capture more particles and so reduced the load on the beam dump. As a positive side effect a narrower vertical aperture would improve the measurement result for the energy spread because the perturbation coefficient becomes smaller as well.

5 Alternative Proposal for LBS Line Design

The proposal for an LBS line with a slit to minimize the vertical beam size for a monochromatic beam depends crucially on the reliability with which the slit can be built. If it will be found out that it is technically impossible to meet the required specifications or the radiation level induced by the activation of the slit becomes too high, then an alternative solution must be found. Therefore, instead of using a slit to reduce the vertical emittance, a second approach has been tested. In this case the beam evolution is manipulated by two quadrupole magnets in front of the spectrometer magnet, so that the vertical beta-function, and so the beam size, at the point of detection is minimized, in case of a monochromatic beam ($dT = 0$). The vertical emittance is left untouched. The energy measurement principle remains the same because the beam is again analyzed by a vertical bending magnet, and mean energy and energy spread are derived from the vertical beam size recorded by a SEM grid.

Another difference to the LBS line with a slit is that the particle distribution is not distorted by an absorptive device. Therefore, the values for mean energy and energy spread can now immediately be measured as they are defined at the entrance to LTB.BHZ40 (Figure 2). Fig. 2

5.1 Layout of the LBS Line with Quadrupole Magnets

The geometrical layout of the experimental zone imposes some constraints for a LBS line with quadrupole magnets. Due to the limited horizontal space available behind the LTB.BHZ40 no quadrupole magnet with typical dimensions of several 10 cm can be put in the first 5200 mm of the line. Furthermore, as now the full beam intensity arrives at the SEM grid a proper beam dump must be integrated into the ceiling of the experimental area because of the vertical trajectory of the beam behind the spectrometer magnet. It is not possible to switch to a horizontal measurement due to the layout of the experimental zone.

The layout of the alternative proposal looks as follows, as before all lengths are referred to the entrance of LTB.BHZ40 (position 0 mm).

- Quadrupole magnet 1 with field gradient $k = -1.0$ T/m at position 6419 mm.

CERN
CH - 1211 Geneva 23
Switzerland

Geneva, 23.02.2010

- Quadrupole magnet 2 with field gradient $k = -1.0\,\mathrm{T/m}$ at position $9181\,\mathrm{mm}$.
- Spectrometer magnet with bending angle $54°$, radius $1500\,\mathrm{mm}$, and edge angles $4.5°$. Its position is at $11475\,\mathrm{mm}$.
- SEM grid $2949\,\mathrm{mm}$ with wire distance $0.75\,\mathrm{keV}$ behind the exit of the spectrometer magnet. This gives an energy resolution of $63.3\,\mathrm{keV}$.

5.2 Simulation Results of the LBS Line with Quadrupole Magnets

The important quantities for a certain proposal derived from the measured SEM grid signal are measured beam sizes for beams with and without momentum spread, perturbation coefficient and vertical dispersion to calculate the energy spread. These main results are summarized in Table 13.

Tab. 13

Beam Size for $\frac{dp}{p} = 0$	$0.5043\,\mathrm{mm}$
Nominal Beam Size	$1.6548\,\mathrm{mm}$
Beam Size Ratio	3.2814
Perturbation Coefficient Δ	0.3200
Vertical Dispersion	$3.115209\,\mathrm{m}$

Table 13: RMS beam sizes (from Path), beam size ratio and perturbation coefficient for the design proposal of the LBS line with quadrupole magnets. The vertical dispersion value is determined at the SEM grid position with TRACE 3-D.

These values are used to calculate the energy spread. In a first attempt the natural beam width is again neglected.

$$\frac{dp}{p} = 5.312 \cdot 10^{-4} \quad \text{and} \quad dT = 156.9\,\mathrm{keV}. \tag{16}$$

The reference value is $149.6\,\mathrm{keV}$ so that the reconstructed values deviates by about 4.9% from the simulated one. Then, if the beam width is corrected for the natural beam width, better results are achieved.

$$\frac{dp}{p} = 5.059 \cdot 10^{-4} \quad \text{and} \quad dT = 149.4\,\mathrm{keV}. \tag{17}$$

The energy spread is now slightly underestimated, but the deviation is reduced by about one order of magnitude to $\approx -0.1\%$. This improvement is numerically correlated to the size of the squared perturbation coefficient $\Delta^2 = 10.2\%$. This value is one order of magnitude higher than for the LBS with slit design. Therefore, only if the full equation 1 is used to calculate the energy spread, the LBS line with quadrupole magnets becomes competitive with the LBS line with slit proposal. The implication is that the values of β and ε must be derived from simulations or complementary measurements so that further error sources must be respected.

Fig. 10 The results for the absolute energy measurements are illustrated in Figure 10.

Fig. 10(a) Fig. 10(b) It is proven that simulations give a correlation between energy and vertical position at the position of the SEM grid with correlation coefficient -95.6% (Figure 10(a)). In Figure 10(b) the same distribution is depicted, but now the data per position bin are averaged and the RMS per bin is calculated. The fitted slope is $85.1\,\mathrm{keV/mm}$, and the error bars per data point represent the energy width sampled on a single wire. It varies between $47\,\mathrm{keV}$ and $50\,\mathrm{keV}$, which can only be reduced if a correction for the contribution of the natural beam width is applied. Otherwise, the intrinsic error is already very close to the SEM grid resolution of $63.3\,\mathrm{keV}$ between two neighboring wires.

Fig. 10(c) Shifting the energy within $\pm\,1\,\mathrm{MeV}$ results again in a linear calibration curve (Figure 10(c)). The errors on the vertical position are relatively small, corresponding to an energy uncertainty of about $31\,\mathrm{keV}$ at maximum. By design of this proposal the particle statistics at the SEM grid is only limited by the number of generated input particles. Therefore, a good quality of the fit is immediately achieved (Figure 10(d)), expressed by this lower energy uncertainty compared to the LBS line with slit proposal.

Fig. 10(d)

CERN
CH - 1211 Geneva 23
Switzerland

Geneva, 23.02.2010

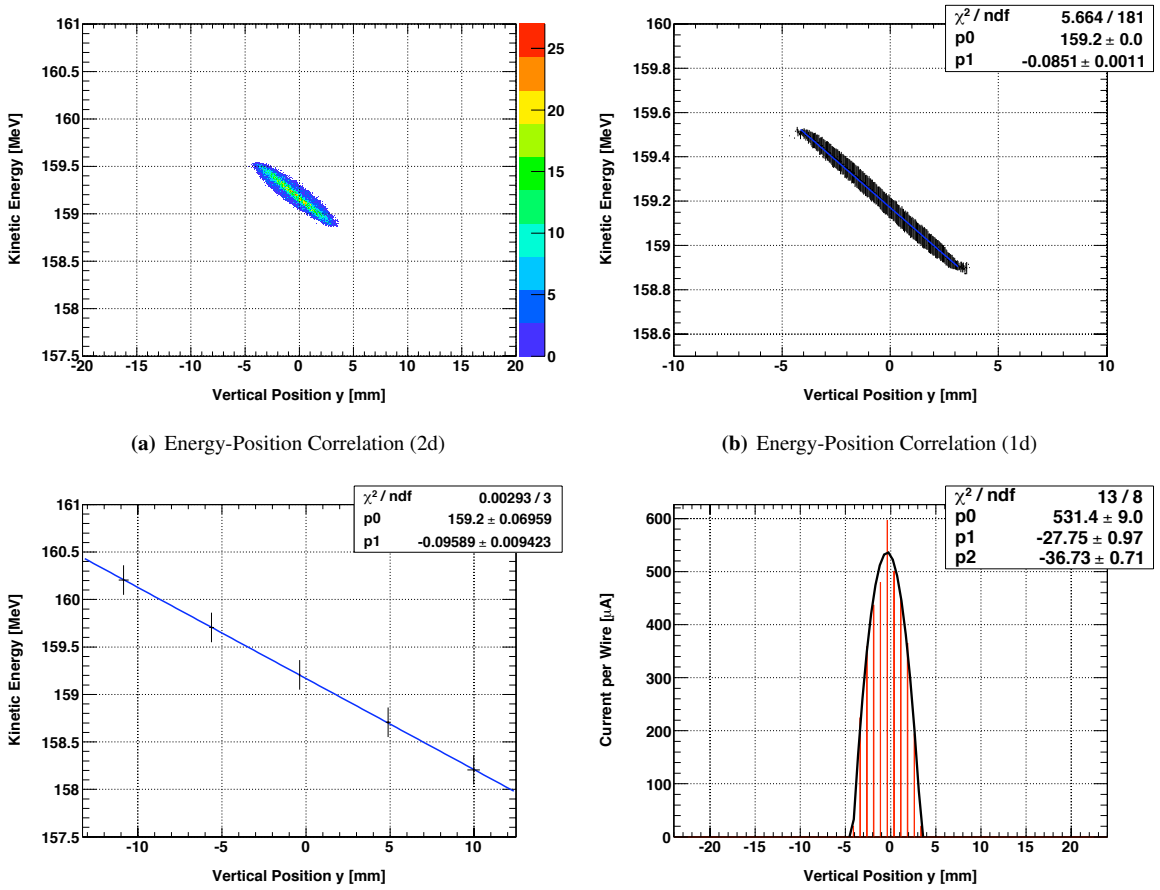

(a) Energy-Position Correlation (2d)

(b) Energy-Position Correlation (1d)

(c) Energy Calibration Curve

(d) Position Distribution

Figure 10: The upper row shows the correlation between energy and vertical position of particles at the SEM grid position (left: 2-dimensional density distribution, right: mean value with RMS error per bin). In the lower row the projection of the two-dimensional distribution to the position axis with a simulation of the discrete SEM grid readout (left), and a linear position calibration curve for beams with shifted kinetic energy values up to ± 1 MeV (right) are displayed.

5.3 Variation of Vertical Beam Parameters

The aim of varying the vertical beam parameters is to check if the perturbation coefficient can be further reduced if the transverse beam parameters α and β are matched to new input parameters at LTB.BHZ40. For that reason the two values are systematically set to one half and twice of its nominal values of $\alpha_0 = 2.520$ and $\beta_0 = 22.978\,\mathrm{mm/mrad}$.

The elements in the line stay the same as above described except for the edge angles of the spectrometer magnet, which are modified such, that for a monochromatic beam the minimum of the vertical beta-function is always located at the SEM grid position. In Table 14 the results are summarized. Tab. 14

If the input parameter can be matched to cited values, then a significant improvement can be achieved, which is almost as good as for the LBS line with the slit ((2), (6), and (7)).

In addition, the sensitivity of the beam size ratio has been investigated, when the SEM grid is slightly displaced by $\pm 50\,\mathrm{mm}$ referred to the optimal position. It can be seen, that the highest increase of the beam size ratio is correlated to a very high sensitivity with respect to position requirements, because the slope of the vertical beta-function close to the local minimum becomes very great. That means, that the gain in performance can be very easily lost, when the line is not accurately aligned or non-simulatable effects degrade the performance by shifting the minimum. In general, there are scenarios with a reliable stability — (1) or even (5) —, where an increase of a factor of almost two can be achieved. In these case the perturbation coefficient is reduced to about 20%, but this is still twice the value of the LBS line proposal with a slit.

CERN
CH - 1211 Geneva 23
Switzerland

Geneva, 23.02.2010

		Edge Angles	R	$\frac{R^-}{R}$	$\frac{R^+}{R}$
(1)	$\alpha = 0.5 \cdot \alpha_0$	5.00°	5.3318	1.0110	0.8659
(2)	$\alpha = 2.0 \cdot \alpha_0$	4.00°	8.0307	0.6334	0.8431
(3)	$\beta = 0.5 \cdot \beta_0$	4.00°	6.9088	0.9328	0.7393
(4)	$\beta = 2.0 \cdot \beta_0$	5.50°	6.3569	0.8251	0.9240
(5)	$\alpha = 0.5 \cdot \alpha_0$ $\beta = 0.5 \cdot \beta_0$	4.50°	4.7530	0.9311	0.9833
(6)	$\alpha = 0.5 \cdot \alpha_0$ $\beta = 2.0 \cdot \beta_0$	5.25°	8.7400	0.6087	0.7448
(7)	$\alpha = 2.0 \cdot \alpha_0$ $\beta = 0.5 \cdot \beta_0$	4.25°	10.9612	0.4552	0.2952
(8)	$\alpha = 2.0 \cdot \alpha_0$ $\beta = 2.0 \cdot \beta_0$	5.00°	2.5278	—	—

Table 14: Results for variable beam parameters at the entrance of LTB.BHZ40. Listed are the modifications of the spectrometer magnet edge angles and the beam size ratio R for the different settings. Furthermore, the beam size ratio for values 50 mm upstream (R^-) and 50 mm downstream (R^+) scaled to the beam size ratio of the optimal position is noted. The last option (8) is not discussed further because it is already worse than the above described.

5.4 LBS Line with Slit compared to LBS Line with Quadrupole Magnets

For both solutions there are two commonalities. On one hand, the layout of the spectrometer magnet is the same except for the edge angle structure, and on the other hand the SEM grid must fulfill the same requirements. Both devices must be newly fabricated, and there is no advantage of one solution over the other. Maybe it must be discussed to reduce the SEM grid wire clearance for the LBS line with quadrupole magnets slightly to respect that the energy width to be measured is 10 keV lower compared to the slit solution. However, this is only a minor modification with only little technical implications.

The biggest advantage of an LBS line with two quadrupole magnets is that the insertion of a slit can be avoided. Thereby the number of objects in the line getting radioactively contaminated during operation is reduced. However, this requires the installation of a beam dump, which can absorb the full beam intensity at the end of the line. As this is not on ground floor level, this could become a very challenging task. For the LBS line with a slit the beam dump at the end of the line does not need to stand the full beam intensity. In addition, the LBS line with quadrupole magnets needs two of these magnets, including their infrastructure, which are surely power supplies, but could include cooling items as well.

From the experimental point of view the slit solution is preferred. First of all, the calculation of a precise value of the energy width depends by less than 1% (compared to 10%) on a correction of the beam size for its natural contribution due to the evolution of the beta-function. Therefore, the correction is not negligible and the measurement of the energy width becomes more independent from simulation codes or additional measurements. Furthermore, the energy interval sampled per SEM grid wire is smaller (RMS width of $13-14$ keV compared to $47-50$ keV). These figures must be compared the total energy width of 160.6 keV and 149.6 keV, respectively, which is intended to be measured. For the LBS line with quadrupole magnets the level of the required resolution of the SEM grid (five measurement points in twice the energy width) is already reached without systematic errors being included, if the measured beam size is not corrected for the contribution of the beta-function.

For the mean energy measurement the slit solution seems to be worse for the shifted energy steps concerning the error on the mean energy. But investigations where the number of sampled particles have been increased show that this can be significantly diminished, especially for a real measurement later on, when high counting rates will be recorded per SEM grid wire.

In summary, it is proposed to select the LBS line design including a slit. Nevertheless, if it is found out during detailed simulations of the required equipment, that this solution can only be fulfilled with unacceptable high efforts it is useful to have a backup solution already available. However, then it is recommended to complement this study with systematic error considerations.

6 Summary

In this report a proposal is presented how to renew the LBS line to measure the mean kinetic energy and the kinetic energy spread of the CERN Linac4 160 MeV H^--beam. The nominal parameters to be measured are $T = 159.2$ MeV and $dT = 160.6$ keV. The measurement principle of this spectrometer line, which is located

CERN
CH - 1211 Geneva 23
Switzerland

Geneva, 23.02.2010

close to the end of the transfer line between Linac4 and PS Booster, is to select a vertical beam slice by a slit, to sort these particles in energy by a vertical spectrometer magnet, and to detect their vertical position with a SEM grid. From the maximum of the recorded signal the mean energy can be derived, while the geometrical width of the signal is proportional to the energy spread. The simulation techniques and several pre-studies are explained before one specific proposal for a new spectrometer line is developed. Its physical parameters and uncertainties with respect to the measurement of mean energy and energy spread of the Linac4 beam are addressed.

At the SEM grid position it is found that vertical position and energy of the particles are strictly correlated (-99.7%) with a slope of $81.9\,\mathrm{keV/\,mm}$. From a second order polynomial fit to the data the maximum position of the signal is determined. Through an optical simulation of the line a calibration curve between maximum position and energy can be generated, and by a precise measurement of the $\vec{B}$-field of the spectrometer magnet the maximum position can be assigned to a mean energy value. The relative precision for the nominal mean energy of

$$\frac{\sigma_T}{T} = 1.8 \cdot 10^{-3}$$

includes fit, systematic and intrinsic uncertainties. The concept of energy painting, i.e. systematic shift of the mean energy by $\pm\,1\,\mathrm{MeV}$ has been simulated as well. With the sufficiently high experimental statistics these shifts can be resolved in time at the order of a few $10\,\mathrm{keV}$ provided the $\vec{B}$-field jitter of the spectrometer magnet is controllable at the level of 0.01%.

The width of the SEM grid signal grid can be used to determine the energy spread provided that the value of the vertical dispersion function at the position of the SEM grid is known from simulation codes like TRACE 3-D for instance. When applying a statistical method (acceptance-rejection method) to the fitted signal, the beam size can reconstructed, and momentum and energy spread can be calculated. This methods yields only a deviation of $-0.2\,\mathrm{keV}$ with respect to the reference value. The error is given by an uncertainty of the acceptance-rejection method, which slightly but systematically underestimates the beam size, errors due to alignment and fabrication precisions of the line, which affect the measured beam size and the knowledge of the vertical dispersion value, and the intrinsic error of the method.

$$\frac{\sigma_{dT}}{dT} = 8.3(8.9) \cdot 10^{-2}$$

The contribution of the natural beam size has been neglected. When this correction is respected, the reconstructed energy spread is only improved on a level of less than $1\,\mathrm{keV}$, but the result becomes additionally dependent on a simulation code or complementary measurements.

The resolution of the SEM gird is degraded due to alignment and fabricating errors by up to almost $10\,\mathrm{keV}$, but can easily be suppressed to only about $1-3\,\mathrm{keV}$ when a good accuracy for the wire distance is achieved.

In the last part an alternative method to measure mean energy and energy spread has been introduced as well. It is based on reducing the vertical beam size at the SEM grid position by beam manipulations with quadrupole magnets instead of using a slit. By definition, this methods does not suffer from a reduced statistical data sample at the SEM grid position, because all particles contribute to the signal. Hence, relatively low errors for the data points of the linear calibration curve between vertical beam center position and mean energy are achieved even for the limited statistical data-set that has been studied.

However, the energy spread sampled per wire is almost $50\,\mathrm{keV}$, so that the intrinsic resolution is almost at the limit of what must be resolved, especially for the energy spread measurement, if the natural beam width is not subtracted. In addition, a correction of the beam size for this natural width becomes indispensable to improve the reconstructed energy spread and to get similar results compared to the LBS line with a slit. Therefore, due to physical but also because of technical reasons, a full beam dump must be installed in the ceiling of the experimental area, the option with the slit is favored so that it is suggested to continue to further follow that design proposal of the LBS line.

Preliminary Functional Specifications

In the following list the functional specifications for the elements required for an LBS line upgrade are given.

- **LTB.BHZ40**
  The current through the magnet coil must be increased to $111\,\mathrm{A}$ to bend the higher energetic into the LBS

CERN
CH - 1211 Geneva 23
Switzerland

Geneva, 23.02.2010

line[8]. The magnet can stand this higher current ($I_{max} = 210$ A), but potentially the power supply must be adapted. Furthermore, as the magnet is water-cooled, it must be verified, if the heat can be dissipated into the existing cooling cycle.

- **Slit**
  The length is currently assumed to be 200 mm, but still subject to a slit design study. It must only be long enough to absorb 160 MeV-H$^-$ ions. The position of the slit is proposed to be between 4089 mm and 4289 mm downstream of the exit of LTB.BHZ40. If the result of simulation study yield a shorter length, then it must be guaranteed that the alignment point of the slit is defined at its exit side. The horizontal aperture is 148 mm, just corresponding to the size of the present beam pipe. The vertical aperture is required to be 1 mm. It has been simulated that an accuracy of 50 µm is acceptable. A variable vertical aperture is an option so that fluctuations of the transmitted current due to changes in the input parameters can be equalized, or to further reduce the vertical beam size to improve the physical performance of the measurement line.

- **Spectrometer Magnet**
  For the spectrometer magnet a compromise between bending angle, resolution and size is chosen. The radius must be 1500 mm and the bending angle 54°. It should be equipped with tilted edges of 10°, so that an edge angle focusing is provided. The beam sizes at the entrance are 5.1 mm × 2.0 mm ($\sigma_{hor.} \times \sigma_{ver.}$), so that a gap vertical gap height of 100 mm seems to be reasonable. The relative error on the $\vec{B}$-field stability is required to be corresponding to the momentum resolution of the line, i.e. $2 \cdot 10^{-4}$. A power supply, and perhaps cooling infrastructure, must be found accordingly. For precisely measuring the $\vec{B}$-field the installation of an NMR probe should be foreseen.

- **SEM Grid**
  It is proposed to install a SEM grid 3375 mm (4139 mm from magnet mid-point) downstream of the exit of the spectrometer magnet with wire clearance 0.75 mm and wire width 0.04 mm. In this configuration the momentum and energy resolutions are 109.5 keV/c and 56.8 keV, respectively. The minimum geometrical dimensions must be ±17 mm to just meet the requirements for longitudinal energy painting of ± 1 MeV. The readout of the SEM grid must time-differentiated with a repetition rate of 1 MHz, which is the ramping rate presently to be resolved. In addition, it must be checked if the SEM grid must be shielded from the beam dump installed further downstream.

  The option to steer the beam always into the center of the SEM grid by synchronously adjusting the field-strength of the spectrometer magnet, when the energy is shifted, so that only the inner part of the SEM grid must be equipped with a highly resolving sensitive area, has been briefly discussed. Even if this would somehow minimize the required readout electronics, the technical realization seem to be too challenging, for instance it is assumed that a ceramic beam pipe is needed to suppress induced currents and thereby to avoid distortions of the $\vec{B}$-field.

- **Beam Dump**
  At the end of the line a beam dump should be built. The simulated beam size at the SEM grid are 3.0 mm × 2.0 mm ($\sigma_{hor.} \times \sigma_{ver.}$) and the angles are 0.6 mrad × 0.7 mrad ($\sigma_{hor.} \times \sigma_{ver.}$). The current to be absorbed is 13 mA for nominal beam design, but can also be 20 mA if the beam input parameters change and the slit is not further closed to absorb more particles. The pulse length should be assumed to be 100 µs.

- **Other Technical Infrastructure**
  Presently, there are three transformers installed in the line, two behind the slit and one behind the spectrometer magnet immediately in front of the SEM grid. It must be checked, if they can be used for the Linac4 beam. But at least one should be kept/replaced behind the slit to measure the transmission through the slit, and a second one behind the spectrometer magnet, so that beam current in both parts of the line can be surveyed.

- **Interlocks**
  A few failure scenarios should be interlocked. All cooled devices should be controlled, so that the line is not used, if any cooling fails. Then, the current of the spectrometer magnet must be restricted to a

[8] There is also the LBE line connected to the same magnet. It has a greater bending angle, so that the minimum acceptable current must be actually 172 A.

CERN
CH - 1211 Geneva 23
Switzerland

Geneva, 23.02.2010

certain operational interval, so that the beam is properly bend towards the SEM grid. As there is no full beam dump at the end of the line it should also be inhibited to use the line, if the radiation level becomes too high. The output of the transformers should be monitored as well, to verify that the line is working according to its intention (particle absorption by slit, all particles are properly transferred through the vertical bending magnet).

- **Software**
  A software application should provide a routine to fit the SEM grid data with a second order polynomial and to simulate random data for the acceptance-rejection method. Other reconstruction techniques have not been tested, but can surely serve as an alternative to obtain the beam size from the fitted data. In any case, the calculating routines must be implemented in a software application.

Acknowledgement

I would like to thank A. Lombardi for her valuable input for the present studies and for explaining so many details about designing a spectrometer line. The physical and technical knowledge on spectrometer line simulations that M. Esraqi and G. Bellodi have shared with me has been and is still highly appreciated. The idea of the alternative approach of building a spectrometer line without a slit has been first brought up by C. Carli. I would like to thank him for intense discussions not only on this topic, but in general on all kinds of results. I am very grateful for the information about the technical details of data taking with SEM grids that U. Raich provided me. Finally, I would like to thank B. Mikulec for proof-reading this document and for her valuable comments.

CERN
CH - 1211 Geneva 23
Switzerland

Geneva, 23.02.2010

A Configuration File for the LBS Line in TRACE 3-D

A.1 LBS Line with Slit

The following TRACE 3-D configuration file describes the LBS line starting behind the slit. The beam input parameters are determined with Path simulations up to the exit of the slit. The SEM grid is virtually located at the end of the drift element CMT(005).

```
&data
 ER = 939.294, Q=-1.0, W=159.16842153283, XI=11.25

 EMITI  =  2.525,  0.283, 1389.880
 BEAMI  = -1.319, 12.695, -0.026, 0.883, 17.146, 4.683

 BEAMCI =  0.0,  0.0, 0.0,  0.0,  0.0, 0.0
 BEAMF  =  0.00000,  0.00000, 0.00000,  0.00000,  0.00000, 0.00000

 FREQ = 352.210, PQEXT = 2.50, ICHROM = 0.0, IBS = 0, XC = 0.00000

 YM  = 5, DPP = 100, DISPR=5

 XMI = 10.0, XPMI =  5.0,  DPMI =  90.0, DWMI = 350
 XMF = 10.0, XPMF =  5.0,  DPMF =  90.0, DWMF = 350
 N1 = 1, N2= 5,  NEL1 = 1, NEL2 = 5, NP1 = 1, NP2 = 6
 SMAX = 5.0, PQSMAX = 2.5, IBS = 0

 CMT(001)=' 6286 Drift   ' NT(001)=  1, A(1, 001)= 6286
 CMT(002)=' 6286 EdgeA   ' NT(002)=  9, A(1, 002)= 10.00, 1500, -100.0, 0.45, 2.8
 CMT(003)=' 7700 Dipole2 ' NT(003)=  8, A(1, 003)= 54.00, 1500,    0.0, 1
 CMT(004)=' 7700 EdgeB   ' NT(004)=  9, A(1, 004)= 10.00, 1500, -100.0, 0.45, 2.8
 CMT(005)='11075 Drift   ' NT(005)=  1, A(1, 005)= 3375
 CMT(006)='12075 Drift   ' NT(006)=  1, A(1, 006)= 1000
&end
```

A.2 LBS Line with Quadrupole Magnets

The following TRACE 3-D configuration file describes the LBS line with quadrupole magnets starting at LTB.BHZ40. The SEM grid is virtually located at the end of the drift element CMT(017).

```
&data
 ER = 939.294, Q=-1.0, W=159.16842153283, XI=65.00

 EMITI  =  3.284,  3.745,  1944.164
 BEAMI  = -0.211,  5.357,  2.520,  22.978,  15.209,  4.038

 BEAMCI =  0.0,  0.0, 0.0,  0.0,  0.0, 0.0
 BEAMF  =  0.00000,  0.00000, 0.00000,  0.00000,  0.00000, 0.00000

 FREQ = 352.210, PQEXT = 2.50, ICHROM = 0.0, IBS = 0, XC = 0.00000

 YM  = 15.0, DPP = 100,  DISPR = 1.0

 XMI = 10.0, XPMI =  5.0,  DPMI =  90.0, DWMI = 0.01
 XMF = 10.0, XPMF =  5.0,  DPMF =  90.0, DWMF = 350

 N1 = 1, N2= 17,  NEL1 = 1, NEL2 = 17, NP1 = 1, NP2 = 18
 SMAX = 5.0, PQSMAX = 2.5, IBS = 0

 CMT(001)='     0 EdgeA   ' NT(001)=  9, A(1, 001)=  0.00, 15000, 100.0, 0.45, 2.8
```

CERN
CH - 1211 Geneva 23
Switzerland

Geneva, 23.02.2010

```
 CMT(002)='   900 Dipole1 ' NT(002)=  8, A(1, 002)=  3.44, 15000, 0.00000, 0
 CMT(003)='   900 EdgeB   ' NT(003)=  9, A(1, 003)=  3.44, 15000, 100.0, 0.45, 2.8
 CMT(004)='  6419 Drift   ' NT(004)=  1, A(1, 004)=  5519

 CMT(005)='  6569 Drift   ' NT(005)=  1, A(1, 005)= 150.0
 CMT(006)='  7031 Quad1   ' NT(006)=  3, A(1, 006)=  -1.0  462.0  0.0  0.0  0.0
 CMT(007)='  7181 Drift   ' NT(007)=  1, A(1, 007)= 150.0

 CMT(008)='  9181 Drift   ' NT(008)=  1, A(1, 008)= 2000

 CMT(009)='  9331 Drift   ' NT(009)=  1, A(1, 009)= 150.0
 CMT(010)='  9793 Quad2   ' NT(010)=  3, A(1, 010)=  -1.0  462.0  0.0  0.0  0.0
 CMT(011)='  9943 Drift   ' NT(011)=  1, A(1, 011)= 150.0

 CMT(012)=' 11475 Drift   ' NT(012)=  1, A(1, 012)= 1532
 CMT(013)=' 11475 EdgeA   ' NT(013)=  9, A(1, 013)=  4.50, 1500, -100.0, 0.45, 2.8
 CMT(014)=' 12889 Dipole2 ' NT(014)=  8, A(1, 014)= 54.00, 1500,    0.0, 1
 CMT(015)=' 12889 EdgeB   ' NT(015)=  9, A(1, 015)=  4.50, 1500, -100.0, 0.45, 2.8

 CMT(016)=' 15838 Drift   ' NT(016)=  1, A(1, 016)= 2750
 CMT(017)=' 16838 Drift   ' NT(017)=  1, A(1, 017)=  199
 CMT(018)=' 16838 Drift   ' NT(018)=  1, A(1, 018)= 1000
&end
```

CERN
CH - 1211 Geneva 23
Switzerland

Geneva, 23.02.2010

List of Figures

List of Tables

CERN
CH - 1211 Geneva 23
Switzerland

Geneva, 23.02.2010

References

[1] CERN Technical Drawings. *Layout Machine Ligne LTB (Sector 2) and references therein*. Available on → https://edms.cern.ch, Document PS LMLTB 8003.

[2] CERN Technical Drawings. *Ligne LTB (LBS Line) and references therein*. Available on → https://edms.cern.ch, Document PS LMLTB 8004.

[3] K. R. Crandall and D. P. Rusthoi. *TRACE 3-D Documentation*, May 1997.

[4] A. Perrin, J.-F. Amand, T. Muetze, and J.-B. Lallement. *Travel User Manual 4.07*, April 2007.

[5] R. Brun and F. Rademakers. Root - an object orientated data analysis framework. In *Nuclear Instruments and Methods in Physics A 389 (1997)*, AIHENP'96 Workshop Lausanne, September 1996, pages 81–86.

[6] G. Bellodi et al. *Updated layout of the LINAC4 transfer line to the PS Booster (Green Field Option)*. CERN-AB-Note-2008-036, 2008.

[7] C. Carli et al. *Active Longitudinal Painting for the H^- Charge Exchange Injection for the Linac4 Beam into the PS Booster*. CERN-AB-Note-2008-011, 2008.

[8] B. Cheymol. *Private Communication*, 2009.

[9] G. Cowan. *Statistical Data Analysis*. Oxford University Press Inc., New York, 1998.

CERN
CH - 1211 Geneva 23
Switzerland

Geneva, 23.02.2010